Title: Muscle molecular adaptations to endurance exercise training are conditioned by glycogen availability: a proteomics-based analysis in the McArdle mouse model

Running head: Proteomic analysis of the McArdle mouse

Authors: Carmen Fiuza-Luces[1*], Alejandro Santos-Lozano[2,3*], Francisco Llavero[4], Rocío Campo[5], Gisela Nogales-Gadea[6], Jorge Díez Bermejo[7], Carlos Balandrón[3], África González-Murillo[8], Joaquín Arenas[1], Miguel A. Martín[1,9], Antoni L Andreu[9,10], Tomàs Pinós[9,10], Beatriz G. Gálvez[2,7], Juan A. López[5,11], Jesús Vázquez[5,11], José L. Zugaza[4,12,13**], Alejandro Lucia[2,7**]

*Contributed equally to this work

**share senior authorship

Affiliations:

[1] Mitochondrial and Neuromuscular Diseases Laboratory and 'MITOLAB-CM', Research Institute of Hospital '12 de Octubre' ('*i+12*'), Madrid, Spain; [2] Research Institute of the Hospital 12 de Octubre ("i+12"), Madrid, Spain; [3] i+HeALTH, European University Miguel de Cervantes, Valladolid, Spain; [4] Achucarro - Basque Center for Neuroscience, Bilbao, Spain; [5] Laboratory of Cardiovascular Proteomics, Centro Nacional de Investigaciones Cardiovasculares Carlos III (CNIC), Madrid, Spain; [6] Research group in Neuromuscular and Neuropediatric Diseases, Neurosciences Department, Germans Trias i Pujol Research Institute and Campus Can Ruti, Autonomous University of Barcelona, Badalona, Spain; [7] Universidad Europea de Madrid, Spain; XX [8] Fundación para la Investigación Biomédica, Hospital Universitario Niño Jesús, and Instituto de Investigación

This is an Accepted Article that has been peer-reviewed and approved for publication in the The Journal of Physiology, but has yet to undergo copy-editing and proof correction. Please cite this article as an 'Accepted Article'; doi: 10.1113/JP275292.

Sanitaria La Princesa, Madrid, Spain.[9] Spanish Network for Biomedical Research in Rare Diseases (CIBERER), Spain;. [10] Neuromuscular and Mitochondrial Pathology Department, Vall d'Hebron University Hospital, Research Institute (VHIR), Autonomous University of Barcelona, Barcelona, Spain; [11] Centro Integrado de Investigación Biomédica en Red en enfermedades cardiovasculares (CIBERCV); [12] Department of Genetics, Physical Anthropology and Animal Physiology, Faculty of Science and Technology, University of the Basque Country, Leioa, Spain; [13] IKERBASQUE, Basque Foundation for Science, Bilbao, Spain.

***First two authors contributed equally to this work**

Corresponding author:

Carmen Fiuza-Luces, PhD

Research Institute of Hospital '12 de Octubre' ('i+12'), Madrid, Spain;

braduxia@hotmail.com

KEY POINTS

. Although they are unable to utilise muscle glycogen, McArdle mice adapt favourably to an individualised moderate-intensity endurance exercise training regime. Yet, they fail reach the performance capacity of healthy mice with normal glycogen availability.

. There is a remarkable difference in the protein networks involved in muscle tissue adaptations to endurance exercise training in mice with/without glycogen availability.

. Indeed, endurance exercise training promoted the expression of only three proteins common to both McArdle and wild-type mice: LIMCH1, PARP1 and TIGD4.

. In turn, trained McArdle mice presented strong expression of mitogen-activated protein kinase 12 (MAPK12).

ABSTRACT

McArdle disease is an inborn disorder of skeletal muscle glycogen metabolism that results in blockade of glycogen breakdown due to mutations in the myophosphorylase gene. We recently developed a mouse model carrying the homozygous p.R50X common human mutation (McArdle mouse), facilitating the study of how glycogen availability affects muscle molecular adaptations to endurance exercise training. Using quantitative differential analysis by liquid chromatography with tandem-mass spectrometry, we analysed the quadriceps muscle proteome of 16-week-old McArdle (n=5) and wild-type (WT) (n=4) mice previously subjected to 8-week moderate-intensity treadmill training or to an equivalent control (no training) period. Protein networks enriched within the differentially expressed proteins with training in WT and McArdle mice were assessed by hypergeometric enrichment analysis. Whereas endurance exercise training improved the estimated maximal aerobic capacity of both WT and McArdle mice as compared with controls, it was ~50% lower than normal in McArdle mice before and after training. We found a remarkable difference in the protein networks involved in muscle tissue adaptations induced by endurance exercise training with/without glycogen availability, and training induced the expression of only three proteins common to McArdle and WT mice: LIM and calponin homology domains-containing

protein 1 (LIMCH1), poly [ADP-ribose] polymerase 1 (PARP1–although the training effect was more marked in McArdle mice), and tigger transposable element derived 4 (TIGD4). Trained McArdle mice presented strong expression of mitogen-activated protein kinase 12 (MAPK12). Through an in-depth proteomic analysis, we provide mechanistic insight into how glycogen availability affects muscle protein signalling adaptations to endurance exercise training.

Keywords: Glycogenosis type V; McArdle disease; proteome; signalling networks; training; exercise.

INTRODUCTION

The importance of endogenous muscle glycogen as a primary fuel source during exertion (particularly for intense endurance bouts) has been a fundamental concept in exercise physiology for half a century (Bergstrom *et al.*, 1967; Pernow & Saltin, 1971). Accordingly, carbohydrate-rich diets have been traditionally recommended for athletes to ensure the replenishment of muscle glycogen stores to meet the metabolic demands of intense training exercise sessions and competitions (Bartlett *et al.*, 2015). However, training with low muscle glycogen availability might induce some beneficial metabolic adaptations in the muscle tissue, including activation of key cell signalling kinases (*e.g.*, protein kinase AMP-activated catalytic subunit alpha 1 [AMPK], p38 mitogen-activated protein kinase [p38MAPK]), transcription factors (*e.g.*, protein 53 [p53], peroxisome proliferator-activated receptor delta

[PPARδ]) and transcriptional co-activators (*e.g.*, peroxisome proliferator-activated receptor-1α [PGC-1α]) (Bartlett *et al.*, 2015), increased fat oxidation (Lane *et al.*, 2015), or delayed liver glycogenolysis (Webster *et al.*, 2016). Elucidating the muscle metabolic adaptations to endurance exercise training as a function of glycogen availability is of interest as it may help to gain insight into the mechanisms that mediate the muscle adaptations to this type of training. This issue can be solved effectively by studying McArdle disease because it allows the investigation of the effects of total unavailability of muscle glycogen on muscle adaptations to endurance exercise training without the need for dietary (*e.g.,* extreme restrictions in carbohydrate intake) or pharmacological manipulations.

McArdle disease (glycogen storage disease type V, OMIM® 232600) is the most prevalent disorder of muscle glycogen metabolism. This autosomal recessive disease is caused by pathogenic mutations (the most common of which is the stop codon mutation p.R50X) in both alleles of the *PYGM* gene (MIM#608455) encoding the skeletal-muscle isoform of glycogen phosphorylase, 'myophosphorylase', which leads to total deficiency of the enzyme (Santalla *et al.*, 2014). Because myophosphorylase catalyses the breakdown of glycogen into glucose 1-phosphate in skeletal muscle fibres, patients are unable to obtain energy from their muscle glycogen stores (Santalla *et al.*, 2014). This disorder provokes 'exercise intolerance' in virtually all affected individuals, which typically manifests in the form of acute crises of undue fatigue and muscle pain and stiffness since childhood (Lucia *et al.*, 2012). Paradoxically, patients who are physically active are less severely affected than their inactive peers (Lucia *et al.*, 2012). Prior non-controlled studies have reported benefits of supervised, moderate-intensity 'aerobic' exercise interventions (60–70% of maximum heart rate) for

patients with McArdle disease, in the form of increased peak oxygen uptake (VO_{2peak}) (Haller *et al.*, 2006; Mate-Munoz *et al.*, 2007) associated with improvements in the muscle levels of two key aerobic enzymes, citrate synthase and beta-hydroxyacyl coenzyme A dehydrogenase (Haller *et al.*, 2006). No other molecular data are, however, available on muscle tissue adaptations to training in these patients.

We recently generated a knock-in mouse model of McArdle disease (mice homozygous for the *pygm p.R50X* mutation) (Nogales-Gadea *et al.*, 2012; Brull *et al.*, 2015). Because this model closely mimics the phenotypes observed in patients (Nogales-Gadea *et al.*, 2012), it can serve as a useful tool to assess the effects of potential treatment interventions for McArdle disease, including endurance exercise training. It was therefore the aim of our study to identify key proteins and pathways involved in the endurance exercise training adaptations at the muscle tissue level in McArdle disease. To do this, we examined, using a controlled design, the effects of submaximal endurance training on the skeletal muscle proteome of wild-type (*wt/wt*) and McArdle (*p.R50x/p.R50x*) mice.

METHODS

Ethical approval

The study received ethical institutional (Centre of Energy, Environment and Technical Research, CIEMAT) review board approval (reference number 179/15). Experiments were carried out according to the guidelines laid down by the institution's welfare committee, and conformed to the principles and regulations as described by Grundy (Grundy, 2015). All

procedures were carried out according to European and Spanish legislative and regulatory guidelines (European convention ETS 1 2 3, on the use and protection of vertebrate mammals in experimentation and for other scientific purposes, and Spanish Law 32/2007, and R.D. 1201/2005 on the protection and use of animals in scientific research). The investigators of the present study understand the ethical principles under which the *Journal of Physiology* operates and our work complies with its animal ethics checklist. Whenever possible, efforts were made to minimise animal discomfort (see '*Endurance exercise training intervention in McArdle and wild-type mice'*).

Animals

Founder *p.R50X/p.R50X* knock-in mice of mixed genetic background (Nogales-Gadea *et al.*, 2012) were backcrossed onto the wild-type CB7Bl/6J background for ten generations. All the animals were genotyped with LoxP-F and LoxP-R as previously reported (Nogales-Gadea *et al.*, 2012).

A total of 36 male mice (age: 8 weeks; wild-type: n=18; McArdle: n=18) were housed in Eurostandard type IIL microisolator cages (five mice maximum in each) under controlled conditions of temperature and humidity (20°C ± 2°C and 55% ± 10%, respectively) at the animal facility of the CIEMAT (registration no. ES280790000183, Madrid, Spain). The cages were lit (fluorescent lighting) from 7:00 a.m. to 7:00 p.m., and food (Harlan Teklad Global Diets 2914) and water (50 μm filtered and UV irradiated) were provided *ad libitum*.

Study design and endurance exercise training intervention

Pre-training phase

Mice were allowed to adapt to the treadmill (Harvard Apparatus; Panlab, Barcelona, Spain) in three sessions (on three separate days) as described (Fiuza-Luces *et al.*, 2013); adaptation involved a gradual increase in running time, treadmill velocity and inclination, starting with placement of the mouse on the treadmill with movement at a very low speed during the first day (0% inclination and 0–5 cm s^{-1} speed for 1 min, with 0.1 mA electrical stimulation) and ending with a 20-min period at low running intensity on the third day (15% and 12 cm s^{-1}, electrical stimulation 0.1 mA, 1 Hz, 200 ms). A total of four treadmills were used and each mouse was consistently trained and tested on the same treadmill.

Maximal endurance exercise performance test

Once the mice had adapted to the treadmill, they were subjected to a gradual test until exhaustion to determine total running distance as a proxy of their maximal aerobic capacity (Hoydal *et al.*, 2007). The test was performed after a warm-up period of 20 min at a speed of 12 cm s^{-1} (with 15% inclination), and followed a previous protocol from our group with slight modifications in workload increases (Fiuza-Luces *et al.*, 2013). Thus, the initial velocity was 5 cm· s^{-1}, and this was followed by workload increases of 3 cm s^{-1} every 2 min until exhaustion, while treadmill inclination was kept constant at 15% during the whole test and use of electrical stimulation electrical stimulation (0.1 mA, 1 Hz, 200 ms). Mice were defined as exhausted when they spent more than 5 continuous seconds on the electric grid and were unable to continue running at the next speed (Ayala *et al.*, 2009).

Group assignment

McArdle mice were paired-matched based on the total running distance they reached during the aforementioned test, and each pair was randomly assigned to an exercise (n=9, subjected to an 8-week exercise training program) or a control ('sedentary') group (n=9, allowed to freely move in the cage, but not performing the program). The same method of group (exercise or control) assignment and number of animals per group was applied for wild-type mice.

Endurance exercise training intervention in McArdle and wild-type mice

Training load over a period of time is the result of the combination of frequency, duration and intensity of the different sessions. Thus, for the training loads of the two McArdle and wild-type exercise groups during the 8-week period to be comparable despite their different fitness level at baseline, we ensured that the weekly frequency of training sessions and the duration and relative intensity (the latter expressed as % of the velocity reached at the end of the tests [V_{max}]) of each session was the same for the two groups. Thus, the intervention in both exercise groups included 5 weekly sessions (from Monday to Friday; session duration, 30–50 min), which was performed between 08.00 am and 12.00 pm. The duration and relative intensity of each session were also the same and increased gradually in the same manner in the two groups, beginning at low workloads in the first session (30 min at 50% of V_{max} and 0% gradient on the first day) and ending with 50 min at 70–75% of V_{max} and 15% gradient at the end of the program (Fiuza-Luces *et al.*, 2013). All the sessions included a warm-up period (15 min at 40% [start of the program] to 50% of V_{max} [end]) and followed by

a cool-down period (5 min at 35% of V_{max}), both at the same treadmill slope used for the core part.

Whenever possible, efforts were made to minimise animal discomfort. Thus, only gentle tail touching was used to prompt the mice to run and no electrical stimulation was applied during the training sessions. In addition, because carbohydrate ingestion 30–40 min prior to exercise attenuates the risk of muscle damage in McArdle disease (Lucia *et al.*, 2008) and thus for ethical reasons, during the hour before each session McArdle mice were fed one Fruit Crunchies™ pellet (weight, 190 mg; 52% energy from carbohydrate, 20.2% protein, 11.5% fibre, 6.3% fat, 5.1% ash and <10% moisture) (Bio-Serv™, LBS Serving Biotechnology, UK). We verified that all exercise sessions started after the mice had eaten the pellet (which consistently took ≤ 60 min). Ingestion of pellets was chosen instead of parenteral administration of glucose to minimise animal discomfort. To ensure similar conditions in all groups, all the study mice also consumed the aforementioned pellet at the same time of the day.

Post-training phase

At the end of the endurance exercise training program, all animals repeated the aforementioned performance test. Finally, 48 hours after the last test, mice were killed by intraperitoneal injection with a lethal dose of Avertin (0.2%, 0.15 ml g^{-1}). We dissected the *quadriceps* muscles, trimmed of connective tissue, which were immediately snap-frozen in liquid nitrogen before storage at -80^{0}C for proteomics analysis. We chose the *quadriceps* instead of other limb muscles (*tibialis anterior*, *extensor digitorum longus*, or *soleus*) based on its high glycolytic phenotype, for technical reasons (*i.e.*, large size, allowing sufficient

amount of sample for present and future investigations), and also on its use in recent research from our group aiming at identifying molecular markers of important cell functions (energy-sensing pathways, oxidative phosphorylation and autophagy/proteasome systems, oxidative damage, and sarcoplasmic reticulum Ca^{2+} handling) in McArdle mice (Fiuza-Luces *et al.*, 2016).

Paired comparisons were made between the maximal distance measured before and after the training period in the exercise and control group, in both McArdle and wild-type mice (Wilcoxon test). Analyses were performed with Stata statistical software (version 13, Stata Corp; College Station, TX) for MAC. Statistical significance level was set at $p<0.05$.

Proteomic analysis

Proteomic analysis was performed in 10 McArdle (5/group) and 8 wild-type (4/group) mice.

Sample preparation

Muscle samples were extracted in lysis buffer (2% SDS, 10 mM Tris(2-carboxyethyl) phosphine hydrochloride (TCEP) and 50 mM Tris-HCl, pH 7.5) by homogenising the tissue with 3 cycles at 6,500 rpm for 60 s each using a MagNA Lyser Instrument (Roche; Mannheim, Germany). Thereafter, samples were boiled for 5 min and incubated for 30 min at room temperature with agitation. Samples were centrifuged at 15,000 rpm for15 min, and protein concentration in the supernatant was determined with a Direct Detect IR spectrometer (Millipore Ibérica; Madrid, Spain).

Protein digestion and isobaric labelling

For the quantitative differential analysis by liquid chromatography with tandem mass spectrometry (LC-MS/MS) using isobaric tags (TMT 10-plex), ~100 μg of total proteins were digested using the fast and secure (FASP) protocol as previously described with minor modifications (Cardona *et al.*, 2015). Proteins were diluted in 7 mM urea and 0.1 mM Tris-HCl (pH 8.5) (UA) and loaded onto 10 kDa centrifugal filter devices (NanoSep 10k Omega, Pall Life Sciences; Port Washington, NY). The buffer was replaced by washing filters with UA, and proteins were then alkylated using 500 mM iodoacetamide (IAA) in UA to 50 mM IAA for 30 min in the dark. The excess of alkylating reagent was eliminated by washing three times with UA and three additional times with 50 mM ammonium bicarbonate. Proteins were digested overnight at 37°C with modified trypsin (Promega Biotech Ibérica; Alcobendas, Madrid, Spain) in 50 mM ammonium bicarbonate at 30:1 protein:trypsin (w/w) ratio. The resulting peptides were eluted by centrifugation with 50 mM ammonium bicarbonate (twice) and 0.5 M sodium chloride. Trifluoroacetic acid (TFA) was added to a final concentration of 1% and the peptides were desalted onto C18 Oasis-HLB cartridges (Waters; Milford, MA) and dried-down for further analysis.

For stable isobaric labelling, the resulting tryptic peptides were dissolved in 100 mM tri-ethyl-ammonium bicarbonate (TEAB) buffer, and the peptide concentration was determined by measuring amide bonds with the Direct Detect system (Millipore Ibérica). Equal amounts of each peptide sample were labelled using 10-plex TMT Reagents (Thermo Fisher Scientific; Waltham, MA) according to the manufacturer's protocol. Peptides were labelled with TMT reagents previously reconstituted with 70 μl of acetonitrile; after

incubation at room temperature for 2 h, the reaction was stopped with 0.5% TFA, incubated for 30 min, and peptides were combined. Samples were concentrated in a Speed Vac, desalted onto C18 Oasis-HLB cartridges and dried-down for further analysis. To increase proteome coverage, TMT-labelled samples were fractionated by high-pH reverse phase chromatography (High pH Reversed-Phase Peptide Fractionation Kit, Pierce; Rockford, IL) and concentrated as before.

Protein identification and quantitation

Labelled peptides were analysed by LC-MS/MS using a C-18 reversed phase nano-column (75 μm I.D. × 50 cm, 2 μm particle size, Acclaim PepMap RSLC, 100 C18; Thermo Fisher Scientific) in a continuous acetonitrile gradient consisting of 0–30% B in 360 min and 50–90% B in 3 min (A=0.1% formic acid; B=90% acetonitrile, 0.1% formic acid). A flow rate of 200 nl min^{-1} was used to elute peptides from the nano-column to an emitter nanospray needle for real time ionisation and peptide fragmentation on an Orbitrap Fusion mass spectrometer (Thermo Fisher Scientific). An enhanced FT-resolution spectrum (resolution=70,000) followed by the MS/MS spectra from the Nth most intense parent ions were analysed along the chromatographic run. Dynamic exclusion was set at 40 s.

For peptide identification, all spectra were analysed with Proteome Discoverer (version 2.1.0.81, Thermo Fisher Scientific) using SEQUEST-HT (Thermo Fisher Scientific). For database searching at the Uniprot database containing all sequences from mouse and contaminants (April 27, 2016; 48,644 entries), the parameters were selected as follows: trypsin digestion with 2 maximum missed cleavage sites, precursor and fragment mass tolerances of 2 Da and 0.02 Da, respectively, carbamidomethyl cysteine and TMT

modifications at N-terminal and Lys residues as fixed modifications, and methionine oxidation as dynamic modification. Peptide identification was performed using the probability ratio method (Martinez-Bartolome *et al.*, 2008) and false discovery rate (FDR) was calculated using inverted databases and the refined method (Navarro & Vazquez, 2009) with an additional filtering for precursor mass tolerance of 15 ppm (Bonzon-Kulichenko *et al.*, 2015).

Identified peptides with an FDR equal or lower than 1% FDR were used to quantify the relative abundance of each protein from reporter ion intensities, and statistical analysis of quantitative data was performed using the WSPP statistical model previously described (Navarro *et al.*, 2014). In this model, protein log2-ratios are expressed as standardised variables; that is, in units of standard deviation according to their estimated variances (Zq values).

Functional protein analysis

Functional protein analysis of the whole set of quantified proteins was performed using a novel algorithm, system biology triangle (SBT), developed specifically for the analysis of coordinated protein responses in high-throughput quantitative proteomics experiments (Garcia-Marques *et al.*, 2016). This algorithm correlates the performance of a group of proteins inside of a category (biological process) in terms of their quantitative behaviour (relative abundance); thus, changes can be detected in functional biological processes far beyond individual protein responses. Variations in the abundance of annotated functional categories were visualised by comparing the cumulative frequency (sigmoid) plots of the

standardised variable with that of the normal distribution, as in previous research (Isern *et al.*, 2013). Individual protein changes were also considered for further analysis.

Determination of the differentially expressed proteins

The Kolmogorov-Smirnov test was applied to test if the data followed a normal distribution. Student's *t* test or the Wilcoxon rank-sum test was applied to identify differentially expressed proteins (*i.e.,* 'proteins of interest') between exercise and control groups in both McArdle and wild-type mice. *P*-values were adjusted for multiple comparisons with FDR correction.

Biocomputational analysis of proteomics data

Processing of protein expression data

Murine proteins were converted into the corresponding human equivalent UniProt reviewed protein according to the following steps: i) UniProt ID automatic crossing of the murine proteins with human proteome with corresponding databases [InParanoid (Sonnhammer & Ostlund, 2015) and the Mouse Genome Database (MGD) (Blake *et al.*, 2017)], ii) gene name automatic crossing of the murine proteins with human proteome with corresponding databases [InParanoid (Turk *et al.*, 1990)] and iii) Manual Blast (Altschul *et al.*, 1990), selecting the best reviewed match presenting at least an identity value ≥ 70% and E-value ≤ 10^{-6}.

Molecular characterisation of adaptation to endurance exercise training

Adaptation to endurance exercise training was characterised at the molecular level *via* manual curation of the literature. This characterisation was performed in two steps: in the

first step, we identified the main pathophysiological processes related to 'manifestative' adaptations in the skeletal muscle in response to endurance exercise training ('manifestative' signatures), which were further characterised at the protein level to provide a final list of "condition effector" proteins (hereafter termed "effectors") (**Large Data File**, **part 1**). Hence, effectors are those proteins that, according to the existing literature, have previously been reported to play a critical role in the process of interest for a given study *viz.*, skeletal muscle adaptations to endurance exercise training [databases: PubMed, ScienceDirect and Scopus; key words (and combinations thereof): protein, muscle, physical adaptations, sports, exercise, McArdle´s disease and McArdle].

Contextualisation of the differentially expressed proteins within "adaptation to exercise training" protein network

Effector proteins were used to focus the analysis on the biological condition of interest in the human biological network. The direct interactions (physical interactions or functional relationships) among the differentially expressed proteins (in exercise *vs.* control groups), as well as the interactions between the differentially expressed proteins and the effectors of skeletal muscle adaptations to endurance exercise training, were assessed. Different publically available databases were consulted for the human protein network generation (*e.g.*, Reactome, Molecular INTeraction database (MINT) and BioGrid) (Herrando-Grabulosa *et al.*, 2016; Iborra-Egea *et al.*, 2017).

Mechanistic evaluation of the differentially expressed proteins in relation to endurance exercise training: artificial neuronal networks analysis

The possible molecular relationship between the differentially expressed proteins and skeletal

muscle adaptations to endurance exercise training was evaluated by means of artificial neuronal networks (ANNs), following TPMS technology protocols (Herrando-Grabulosa *et al.*, 2016; Iborra-Egea *et al.*, 2017). This approach involves the generation of mathematical models of the biological processes through the use of artificial intelligence techniques. Then, mathematical models were solved by ANNs, which are supervised algorithms that identify relationships between the different nodes in the network. ANN analysis yields a score for each differential protein based on the validations of the prediction capacity of the mathematical models towards known drugs and diseases, as described in databases. The higher the score, the stronger is the predicted mechanistic relationship between the evaluated protein and the biological process. Each score is associated with a *p*-value that describes the probability of the result being a true positive one. Aiming to facilitate the understanding of the results, the obtained scores were divided in three categories: >76, strong ($p<0.05$); 40–76, medium-strong ($p=0.05$–0.25); <40, weak ($p>0.25$).

Proteins presenting 200+ interactions ('sticky proteins'), or proteins that do not have reported interactions, were not included in the topology as they may disrupt the correct assessment of existing relationships (Pache *et al.*, 2008). Relationships between the differentially expressed proteins and skeletal muscle adaptations to endurance exercise training were assessed both for individual proteins and for combinations of two proteins; thus, from all the reported protein interactions, the most interesting are those presenting a synergic effect. The synergy criteria were applied according to the approach described by Berenbaum (Berenbaum, 1989), in which a significant synergic effect is considered when the overall effect is >20% of the sum of the individual effects of the two proteins.

Visualisation of the protein network

Cytoscape 3.5.1. software was used to study the representation of all the reported interactions (both from the significantly associated proteins and nonsignificantly associated proteins) according to the ANN score.

Enrichment analysis

The pathways and biological processes enriched within the differentially expressed proteins in the exercise and control groups within both McArdle and wild-type mice were assessed using a hypergeometric enrichment analysis approach (Rivals *et al.*, 2007). Specifically, the enrichment was run over several sets of proteins, including: Gene Ontology (GO) terms (Biological Process, Cellular Component, Molecular Function) according to European Molecular Biology Laboratory (EMBL)-European Bioinformatics Institute (EBI)/UniProt-GO (The UniProt, 2017); pathways from the Kyoto Encyclopedia of Genes and Genomes (KEGG) (Kanehisa *et al.*, 2014), the Pharmacogenomics Knowledgebase (PharmGKB) (Whirl-Carrillo *et al.*, 2012) and the Small Molecule Pathway Database (SMPDB) (Frolkis *et al.*, 2010); pathological conditions, signatures and pathways from the Biological Effectors Database (BED) (Iborra-Egea *et al.*, 2017) and the regulatory molecular mechanisms included in Transcriptional Regulatory Relationships Unraveled by Sentence-based Text-mining (TRRUST) database (Han *et al.*, 2015). Only those pathways that showed a statistically significant presence were presented (FDR p-value <0.05).

RESULTS

The training loads were common to both McArdle and wild-type exercise groups over the 8-week period and are shown in detail in **Large Data file**, **part 2.** The endurance exercise training program was successful in inducing a significant improvement in the total running distance of both McArdle [141 (31) metres (pre-training) *vs.* 167 (48) metres (post-training); Wilcoxon test p=0.035] and wild-type [275 (30) *vs.* 353 (146) metres, p=0.041] mice, whereas no significant change was found during the same time period in their sedentary controls [140 (41) *vs.* 116 (48) metres, p=0.129 for McArdle and 302 (85) *vs.* 296 (103) metres, p=0.726 for wild-type mice]. Although the relative improvement in total running distance did not differ between McArdle and wild-type mice (Mann-Whitney test p=0.111), the total running distance of McArdle mice was ~50% lower than that of wild-type mice both before and after the endurance exercise intervention. Individual data (total running distance) of the mice used for proteomic analyses are shown in **Figure 1**. When expressed as V_{max}, the test results were as follows: McArdle, exercise group: 26 (3) $cm \cdot s^{-1}$ (pre-training) *vs.* 29 (4) $cm \cdot s^{-1}$ (post-training), Wilcoxon test p=0.054; wild-type, exercise group: 36 (6) (pre-training) *vs.* 41 (8) $cm \cdot s^{-1}$ (post-training), p=0.028; McArdle, sedentary control group: 26 (4) *vs.* 24 (5) $cm \cdot s^{-1}$, p=0.123; wild-type, sedentary control group: 38 (5) *vs.* 37 (7) $cm \cdot s^{-1}$, p=0.180.

The body mass of the mice showed an increasing trend over time irrespective of genotype or intervention (exercise or control): (i) McArdle, exercise group: 20.8 (1.4) g (pre) and 22.0 (1.3) g (post) Wilcoxon test p=0.997; (ii) McArdle, control group: 20.8 (1.3) g (pre) and 22.1 (0.81) g (post), p=0.031; wild-type, exercise group: 18.7 (2.0) g (pre) and 21.3 (1.0)

g (post), p=0.083; wild-type, control group: 19.0 (1.9) g (pre) and 21.7 (2.1) g (post), p=0.805.

Proteomics

Proteins of interest

Data provided by whole proteomic analysis regarding differential proteins within the sedentary and the trained groups of McArdle and wild-type mice, respectively, were analysed by applying Student's t test and the Wilcoxon rank-sum test. A total of 74 differentially expressed proteins between the trained and sedentary wild-type mice and 123 differentially expressed proteins between the trained and sedentary McArdle mice were found (**Large Data File**, **part 3**). Of these differentially expressed proteins in response to endurance exercise training, only three were common to wild-type and McArdle mice: LIM and calponin homology domains-containing protein 1 (LIMCH1); poly (ADP-ribose) polymerase 1 (PARP-1, also known as NAD+ ADP-ribosyltransferase 1 or poly (ADP-ribose) synthase 1); and tigger transposable element derived 4 (TIGD4). Expression of all three proteins was higher in endurance exercise training than in untrained conditions, in both wild-type and McArdle mice; however, statistical significance was not reached for any after FDR adjustment.

Contextualisation of the differentially expressed proteins within exercise training adaptation

The molecular characterisation of the skeletal muscle adaptations to endurance exercise training was carried out through the review of specialised scientific literature. A total of 76 effector proteins were identified and classified into four groups according to their cellular function, such as adaptive muscle growth (14 proteins), muscle angiogenesis (8 proteins),

glucose and lipid metabolism (12 proteins) and mitochondrial biogenesis and remodelling (48 proteins), with 4 of these 76 proteins belonging to two groups (angiogenesis + mitochondrial biogenesis and remodeling) at the same time, cyclic AMP-dependent transcription factor (ATF2), steroid hormone receptor ERR1 (ESRRA, or also ERRa), mitogen-activated protein kinase 12 (MAPK12) and myocyte-specific enhancer factor 2A (MEF2A, or also MEF2); and one, PGC-1α, belonging three groups (adaptive muscle growth + angiogenesis + mitochondrial biogenesis and remodeling) (**Large Data File**, **part 1**).

The role of the differentially expressed proteins in adaptation to endurance exercise training was evaluated according to the molecular characterisation performed. The results of the analysis revealed that only one of the differentially expressed proteins in McArdle mice, MAPK12, had been previously related to skeletal muscle adaptations to exercise training (**Table 1**). MAPK12 is involved both in mitochondrial biogenesis and remodelling and muscle angiogenesis. By contrast, none of the differentially expressed proteins in wild-type mice has previously been reported to play a direct role in skeletal muscle adaptations to endurance exercise training (**Table 2**). However, while only one differentially expressed protein from the two lists (McArdle and wild-type mice) matches the effector proteins defined in the molecular characterisation, it is remarkable that several of them interact with many effectors **(Tables 1** and **2)**. In McArdle mice, ATP synthase H^+ transporting mitochondrial F1 complex gamma polypeptide 1 (ATP5C1), MAPK12 and ATP synthase and H^+ transporting mitochondrial F1 complex epsilon subunit (ATP5E) were related to more than 10 effectors, and proteasome 26S subunit, non-ATPase 14 (PSMD14), integrin-linked kinase (ILK) and chaperonin containing TCP1 subunit 3 (CCT3) interacted with 9 different effectors. While in

wild-type mice, we found that poly(A) binding protein cytoplasmic 1 (PABPC1), protein kinase DNA-activated catalytic polypeptide (PRKDC), ribosomal protein lateral stalk subunit P0 (RPLP0), mitogen-activated protein kinase kinase 4 (MAP2K4) and protein kinase N1 (PKN1) interacted with more than 10 effectors, followed by ribosomal protein L21 (RLP21) interacting with up to 9 different effectors. Additionally, the common differentially expressed protein between the two groups, PARP1, interacted with 7 different effectors, all of them involved in mitochondrial biogenesis and remodelling.

Mechanistic evaluation of the relationship with endurance exercise training: analysis of artificial neuronal networks

The potential molecular relationships between the differentially expressed proteins and skeletal muscle adaptations to endurance exercise training were evaluated through the analysis of mathematical models, to determine the possible activity relationships between protein sets or regions inside the network (*i.e.*, ANN); this allowed us to provide a predictive score that quantifies the probability of the existence of a relationship between the evaluated differential proteins and network region (*i.e.*, the different pathophysiological signatures characterized and adaptation to endurance exercise training as a whole). Each score is associated with a *p*-value that describes the probability of the result being a true positive result. To better understand the results, we divided the ranking score in four categories: strong (*p*-value <0.05), medium-strong (*p*-value 0.05–0.25), weak (*p*-value >0.25) and not assessed. As shown in **Large Data File**, **part 4**, it was not possible to evaluate 5 of 116 proteins for the McArdle mouse groups, and 5 of 73 for the wild-type groups. Nevertheless,

the possible relationship between 111 proteins for McArdle mice and 68 proteins for wild-type mice was successfully assessed. When considering the differential proteins individually, ~28% and 22% of the proteins showed a significant relationship (strong or medium-strong category) with skeletal muscle adaptations to endurance exercise training in McArdle and wild-type mice, respectively. Moreover, when analysing the differential proteins in sets of two proteins, ~30% of the protein combinations showed a significant association with skeletal muscle adaptations to endurance exercise training, both in the McArdle and wild-type mice.

Relationships between the differentially expressed proteins and skeletal muscle adaptations to endurance exercise training: individual protein evaluation

As a result of the analysis of the relationship between individual proteins and skeletal muscle adaptations to endurance exercise training, a total of 33 proteins were reported to present a significant relationship with McArdle disease mice and 16 with wild-type mice (**Table 3**). One of the differentially expressed proteins common to both mouse groups, PARP1, appeared to be significantly related to skeletal muscle adaptations to endurance exercise training. Moreover, the assessment of the potential relationship between the proteins of interest and skeletal muscle adaptations to endurance exercise training signatures allowed the evaluation of specific subsets of the physiological processes that in some cases were not detected by considering the whole context. For instance, 9 proteins of interest in McArdle mice and 5 in wild-type mice that were predicted to be related to at least one of the signatures of skeletal muscle adaptations to endurance exercise training, were actually not found to be related to the general characterisation of skeletal muscle adaptations to endurance exercise training (**Table 3**).

Relationships between the differentially expressed proteins and skeletal muscle adaptations to endurance exercise training: association in combination of two proteins

As a result of the analysis of the relationship between combinations of two proteins and skeletal muscle adaptations to endurance exercise training (**Large Data File**, **part 4**), a total of 2,035 protein combinations were reported to present a significant relationship in McArdle mice and 719 in wild-type mice. When considering only the combinations with a significant synergic effect (synergic effect is considered when the overall effect is >20% of the amount of the individual effect of the two proteins), a total of 199 and 57 protein combinations were found for McArdle and wild-type mice, respectively. One of the common differentially expressed proteins in both groups, LIMCH1, appeared to be significantly related to skeletal muscle adaptations to endurance exercise training in combination with other proteins.

In order to represent the intermolecular relationships obtained regarding protein interactions (**Tables 1** and **2** and **Large Data File**, **part 1**) and mechanistic evaluation (**Large Data File**, **part 4**), a visual protein interaction network map was generated for both McArdle (**Figure 2**) and wild-type (**Figure 3**) mice. Only the proteins with a significant relationship with skeletal muscle adaptations to endurance exercise training (based on ANNs score) and their direct interactions appear on the representations. However, closer analysis of the signalling networks revealed that PARP1 was more profoundly overexpressed in trained McArdle than in trained wild-type mice (**Figures 2** and **3**, respectively).

Enrichment analysis

To analyse the expression data related to signalling pathways and clinical conditions, we

.

undertook a hypergeometric enrichment analysis approach within the differentially expressed proteins in the trained and the control groups of McArdle and wild-type mice. As shown in **Large Data File**, **part 5,** 121 and 79 protein sets were found enriched in the comparison of control *vs.* exercise groups, both in McArdle and wild-type mice. Subsequently, a pathway comparison between the results obtained from both conditions was performed, obtaining 4 common pathways and 117 and 75 proteins specifically enriched in McArdle and wild-type groups, respectively. The enriched protein sets common to McArdle and wild-type conditions corresponded to those related to high blood glucose levels and gene expression (BEDVES database: induction of oxidative stress diabetic neuropathies and induction of oxidative stress diabetic neuropathies and retinopathies; GOFUNTION database: term poly(A) RNA binding and the GOLOCATION referring to cytosol).

The enriched protein sets reported within the differentially expressed proteins in exercise *vs.* control McArdle mice (**Large Data File**, **part 5)** reflect changes related to muscular adaptations to endurance exercise training that may be related to the improvement in exercise tolerance, as well as to processes associated with the pathophysiology of the condition. Regarding enriched protein sets related to muscular adaptations to endurance exercise training, there were several pathways referring to mitochondria and their functions (**Large Data File**, **part 6**), including GO location terms referring to several mitochondrial structures such as the proton-transporting ATP synthase complex (responsible for ATP synthesis), and GO processes such as the respiratory electron transport chain. Furthermore, several pathways and GO terms related to lipid and protein metabolism are also reported in **Large Data File**, **part 6**, and enriched protein sets related to muscle structure and growth are

described in **Large Data File**, **part 7**.

Conversely, the enriched protein sets within the wild-type groups were mainly related to endurance exercise training-induced physiological changes due to focal adhesion, actin cytoskeleton reorganisation and phosphatidylinositol 3-kinase (PI3K) signalling pathway involvement (**Large Data File**, **part 8**). Moreover, several pathways referring to β-blocker activity also appeared to be enriched, possibly due to changes in catecholamine modulation (**Large Data File**, **part 9**).

DISCUSSION

Although McArdle disease causes 'exercise intolerance' (Lucia *et al.*, 2012), under carefully controlled conditions, McArdle patients may perform acute exercise safely, especially if carbohydrate solutions are taken before exercise to bypass the metabolic blockade that occurs upstream of the uptake of glucose by muscle fibres (Vissing & Haller, 2003). They may also adapt favourably to moderate-intensity endurance exercise training (Haller *et al.*, 2006; Mate-Munoz *et al.*, 2007). Yet, no study has assessed in depth the molecular signals associated with muscle exercise adaptations in McArdle patients and how they compare with those of healthy individuals. Accordingly, in the present study we aimed to identify, with no *a priori* hypothesis, the key proteins and protein networks linked to the effects of moderate-intensity endurance exercise training in a mouse model that closely mimics the phenotype of McArdle patients (Nogales-Gadea *et al.*, 2012). Unravelling the muscle metabolic adaptations to endurance exercise training with no muscle glycogen availability might help to gain

insight into the proteome profile that characterises muscle adaptations to such type of training. This is an important question given that the skeletal muscle contains 50–75% of all the body proteins and is responsible for 30–50% of the whole body protein translation process (Frontera & Ochala, 2015). The majority of proteins identified here both in McArdle and wild-type mice control the expression of a myriad of genes related to angiogenesis, carbohydrate, lipid and protein metabolism, mitochondrial biogenesis and remodelling, and muscle growth.

In addition to reporting the first non-pharmacological intervention in this mouse model, a novel finding of our study was that, like patients, McArdle mice adapt favourably to an individualised moderate-intensity endurance exercise training regimem (albeit without reaching the performance capacity of healthy mice). Yet, our results revealed a remarkable difference in the protein networks involved in the muscle tissue adaptations that occur with endurance exercise training with normal glycogen availability (wild-type mice) as compared with those that occur in conditions of blocked glycogenolysis (McArdle mice). Indeed, endurance exercise training promoted the expression of only three proteins common to both McArdle and wild-type mice: LIMCH1, PARP1 and TIGD4. Likely, all three proteins play a prominent role in the relationship between skeletal muscle plasticity and endurance exercise training, independent of muscle glycogen availability, which warrants further investigation. It is well known that during exercise, numerous stress signals are transduced to activate intracellular signalling pathways controlling skeletal muscle gene transcription and translation (Bassel-Duby & Olson, 2006; Koulmann & Bigard, 2006; Favier *et al.*, 2008; Russell, 2010). Against this background, both LIMCH1 and PARP1 could participate in

stress pathways controlled by exercise. Indeed, cell contraction accelerates when LIMCH1 promotes the assembly of actin stress fibres during cell spreading. Moreover, the absence of LIMCH1 expression impacts the formation of actin stress fibres as well as the stability of focal adhesions (Lin *et al.*, 2017), which are fundamental structures in the union of muscle fibres to ensure optimal contraction and muscular distention. TIGD4 protein belongs to the tigger subfamily of the pogo superfamily of DNA-mediated transposons in humans. The latter proteins are related to DNA transposons found in fungi and nematodes and more distantly to transposases Tc1 and mariner, and they are very similar to the major mammalian B centromere protein. However, the exact function of TIGD4 remains to be clarified.

PARP1 is the most characterised member of the PARP family of nuclear enzymes. These proteins are sensitive to changes in intracellular redox pathways, positioning the poly ADP-ribosylation (PARylation) reaction as an important biochemical marker of oxidative stress (Jungmichel *et al.*, 2013). Whereas basal activity of PARP1 is crucial to maintain cellular homeostasis, its over-activity leads to an increase in protein PARylation, which in turn depletes intracellular NAD^+ levels, leading to cell death (Ha & Snyder, 1999). Thus, PARP1 activity is a key sensor for cell survival. Interestingly, we found that endurance exercise training mediates the expression of PARP1 in both McArdle and wild-type mice, although being higher in trained McArdle than in trained wild-type mice. This could be due, at least partly, to increased muscle damage that characterises this disease.

In general, the low overlap between groups (74 and 123 differentially expressed proteins with training in wild-type and McArdle mice, respectively) suggests considerable

differences in the physiological adaptations to chronic endurance exercise between McArdle and wild-type mice, at a mechanistic level. Indeed, when we compared the protein profile between McArdle and wild-type mice after training, we found that McArdle mice presented a specific and strong expression of MAPK12 and a potentially substantial number of effector interactions. MAPK12 is a serine/threonine kinase that acts as an essential component of the MAP kinase signal transduction pathway. Also known as p38MAPKγ, MAPK12 is one of the four p38 MAPKs that play an important role in the cellular response cascade induced by extracellular stimuli such as proinflammatory cytokines or physical stress (Cuenda & Rousseau, 2007). MAPK12 plays a role in myoblast differentiation, as it is involved in the regulation of the expression of the solute carrier family 2 (facilitated glucose transporter), member 1 (SLC2A1). Further, basal glucose uptake in L6 myotubes and MAPK12-signalling positively regulate the expansion of transient amplifying myogenic precursor cells during muscle growth and regeneration (Ho *et al.*, 2004). Our analyses suggest that MAPK12 is also related to mitochondrial biogenesis and remodelling, with such potentially MAPK12-mediated improvement in mitochondrial function perhaps endeavouring to compensate for the deficit in energy supply owing to glycogen unavailability. By contrast, we detected a lower endurance exercise training-induced increase in MPAK12 protein expression in wild-type mice.

Hypergeometric analysis of the highly and significantly expressed proteins in McArdle and wild-type mice (121 and 79 proteins, respectively) provided an enrichment in clinical processes that are related to the induction of oxidative stress, neuropathies and retinopathies. When McArdle and wild-type mice were analysed separately, we observed that

after endurance exercise training in McArdle mice the most widely represented functions were those involved in ATP synthesis and electron transport chain processes, β-oxidation of lipids, and different steps in lipid and protein catabolism. In addition, cell death and regulation of necrotic processes were also reflected in this analysis. In fact, the overexpression of PARP1 could be associated with rhabdomyolysis, and PARP activation is linked to necrosis, as shown in PARP-deficient mouse fibroblasts (Ha & Snyder, 1999). All of the aforementioned adaptations found in McArdle mice after endurance exercise training may be related to the metabolic strategies that the skeletal muscle tissue of McArdle mice deploys to obtain energy. Conversely, after endurance exercise training the functions that were most represented in wild-type mice were those related to cytoskeleton regulation and focal adhesions, and also PI3K and mTOR signalling pathway activation related to maintenance of skeletal muscle cell survival. Thus, from an overall perspective, it seems that the main muscle molecular adaptations to endurance exercise training in McArdle mice are more oriented to obtain energy for tissue *regeneration* in a state of energetic deficit, whereas wild-type muscle adaptations seem to be more related to support tissue *maintenance* while coping with exercise stress stimuli.

Our study is not without limitations. In contrast to human research, where performing repeated muscle biopsy sampling may be feasible, a first technical limitation is the impossibility to determine muscle glycogen content before and after a training session in the wild-type mice as a proof-of-concept for glycogen utilization. Of note, owing to the total inability to utilize glycogen as a fuel, massive muscle glycogen accumulation occurs in McArdle mice, a phenomenon much more remarkable than in patients, with muscle glycogen

levels being several orders of magnitude higher than in CB7Bl/6J wild-type mice as used here (Nogales-Gadea *et al.*, 2012). Moreover, we chose forced treadmill running rather than wheel running as a model of endurance exercise training. Although wheel running is a less stressful, more natural form of activity in rodents, it does not allow for the establishment of predetermined training loads, which was a crucial aspect of our design to ensure they were similar in the exercise groups. Nevertheless, researchers in charge of mouse training were well experienced in mouse handling such as to minimize stress in these animals. Indeed, only gentle tail touching was used to prompt the mice to run and no electrical stimulation was applied during the training sessions. Another potential limitation comes from the use of a single muscle type, *quadriceps* (with a highly glycolytic phenotype) for proteome analyses. Future research should determine whether comparable findings are obtained in a more oxidative muscle like the *soleus* or even in other glycolytic muscles. In this regard, although there are differences between muscles (even between those with a similar metabolic phenotype and with only subtle differences in proportion of fibre types, like the *quadriceps* and *tibialis anterior*) overall, both fast and slow-twitch muscles in the untrained state are affected by both structural degeneration and energy deficiency in McArdle mice (Krag *et al.*, 2016a). Along this line, recent research has identified the *quadriceps* muscle as having more compensatory adaptations to counterbalance energetic deficiency in the untrained state (*i.e.*, in terms of expression of proteins involved in glucose uptake, glycogen synthesis and glycolysis) than other studied muscles, whether they were predominantly glycolytic (*tibialis anterior*, *extensor digitorum longus*) or more oxidative (*soleus*) (Krag *et al.*, 2016b). Finally, we did not report blood serum creatine kinase levels (as an indirect marker of muscle damage) over the study period.

.

In conclusion, we have determined that, akin to patients, McArdle mice responded favourably to moderate-intensity endurance exercise training, although their maximal aerobic capacity is clearly lower than that of normal peers. This suggests that glycogen availability is crucial for ensuring maximal endurance performance in mammals, with unavailability of this substrate resulting in muscles adopting a remarkably different 'molecular strategy' to cope with the training loads while ensuring cellular homeostasis during a state of energetic deficit. In this regard, we have identified for the first time the signalling strategies (in terms of signalling molecules and protein networks) that skeletal muscle employs to overcome blockade of glycogen breakdown during endurance exercise training, demonstrating that the protein network involved in muscle adaptations to such type of training greatly differs depending on glycogen availability (see also **Figure 4** for a summary). Our findings provide a framework for future studies aimed at elucidating the molecular mechanisms associated with the most relevant identified proteins here. It would also be interesting to study in depth some of the proteins sets identified by the enrichment analysis; among which, PARP1, LIMCH1 and MAPK12 emerge as good candidates.

Additional information

Competing interests and Funding

All the authors declare they have no conflict of interesting.

The CNIC is supported by the Ministry of Economy, Industry and Competitiveness (MEIC) and the Pro CNIC Foundation, and is a Severo Ochoa Centre of Excellence (SEV-2015-0505). This study was funded by grants from *Fondo de Investigaciones Sanitarias*

.

(PI15/01756, PI15/00558, PI12/00914, and PI14/00903), cofinanced by FEDER. Gisela Nogales-Gadea is supported by a Miguel Servet research contract (ISCIII CD14/00032 and FEDER) and Carmen Fiuza Luces by a Sara Borrell post doc contract (CD14/00005).

We thank Dr. Kenneth McCreath for his editorial assistance during manuscript preparation.

Author contributions

The experiments were performed in: Centre of Energy, Environment and Technical Research, CIEMAT (mouse genotyping, housing, and training); Centro Nacional de Investigaciones (Cardiovasculares): proteomics.

All authors qualify for authorship (see below) approved the final version of the manuscript and agree to be accountable for all aspects of the work in ensuring that questions related to the accuracy or integrity of any part of the work are appropriately investigated and resolved.

CFL: conception and design of the work + acquisition, analysis and interpretation of data for the work + drafting the work; ASL, JLZ: design of the work + analysis and interpretation of data for the work + drafting the work; FL, JA, MAM, ALA, TP, BGB, JV: interpretation of data for the work + revising the work critically for important intellectual content; GNG, JDB, RC, AGM: acquisition of data for the work + revising the work critically for important intellectual content; CB: analysis and interpretation of data for the work + revising the work critically for important intellectual content; JAL: analysis and interpretation of data for the work + revising the work critically for important intellectual content; AL: conception and design of the work + analysis and interpretation of data for the work + drafting the work.

Figure legends

Figure 1. Individual responses during the intervention period in maximal distance during a gradual treadmill running test until exhaustion in mice used for proteomic analysis.

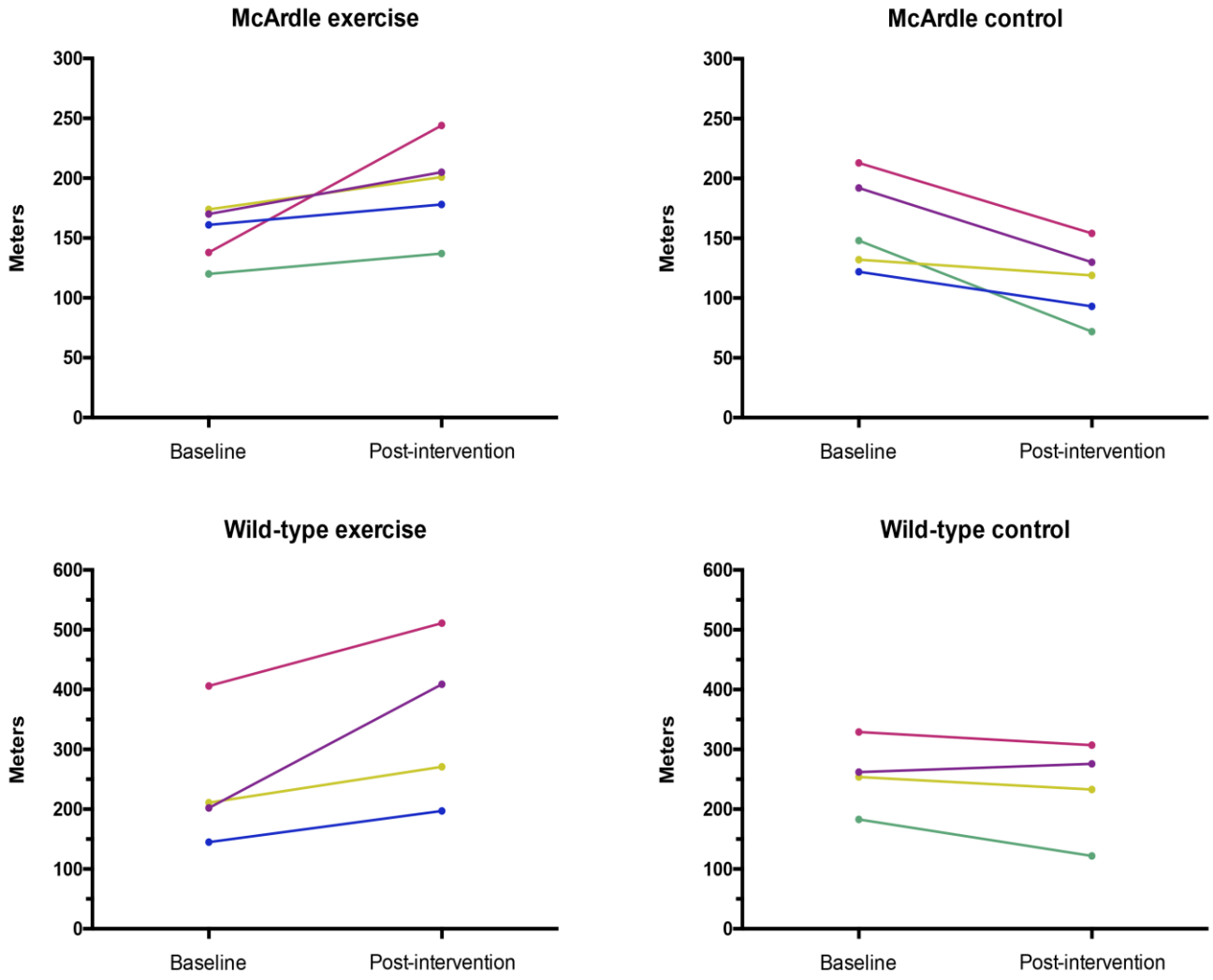

Figure 2. Visual protein interaction network map of the proteins significantly related to skeletal muscle adaptations to endurance exercise training according to the artificial neuronal network (ANN) score, and their interacting proteins, in McArdle (*p.R50X/p.R50X*) mice. The network map includes three representations of the following interactions: i) within the differentially expressed proteins (ovals), ii) between the differentially expressed proteins and skeletal muscle adaptions to endurance exercise effectors (ovals and triangles), and iii) within the skeletal muscle adaptations to endurance exercise effectors (triangles). Note: all the *interactions*, both from the significantly associated proteins and nonsignificantly associated proteins according to the ANN score, are reported

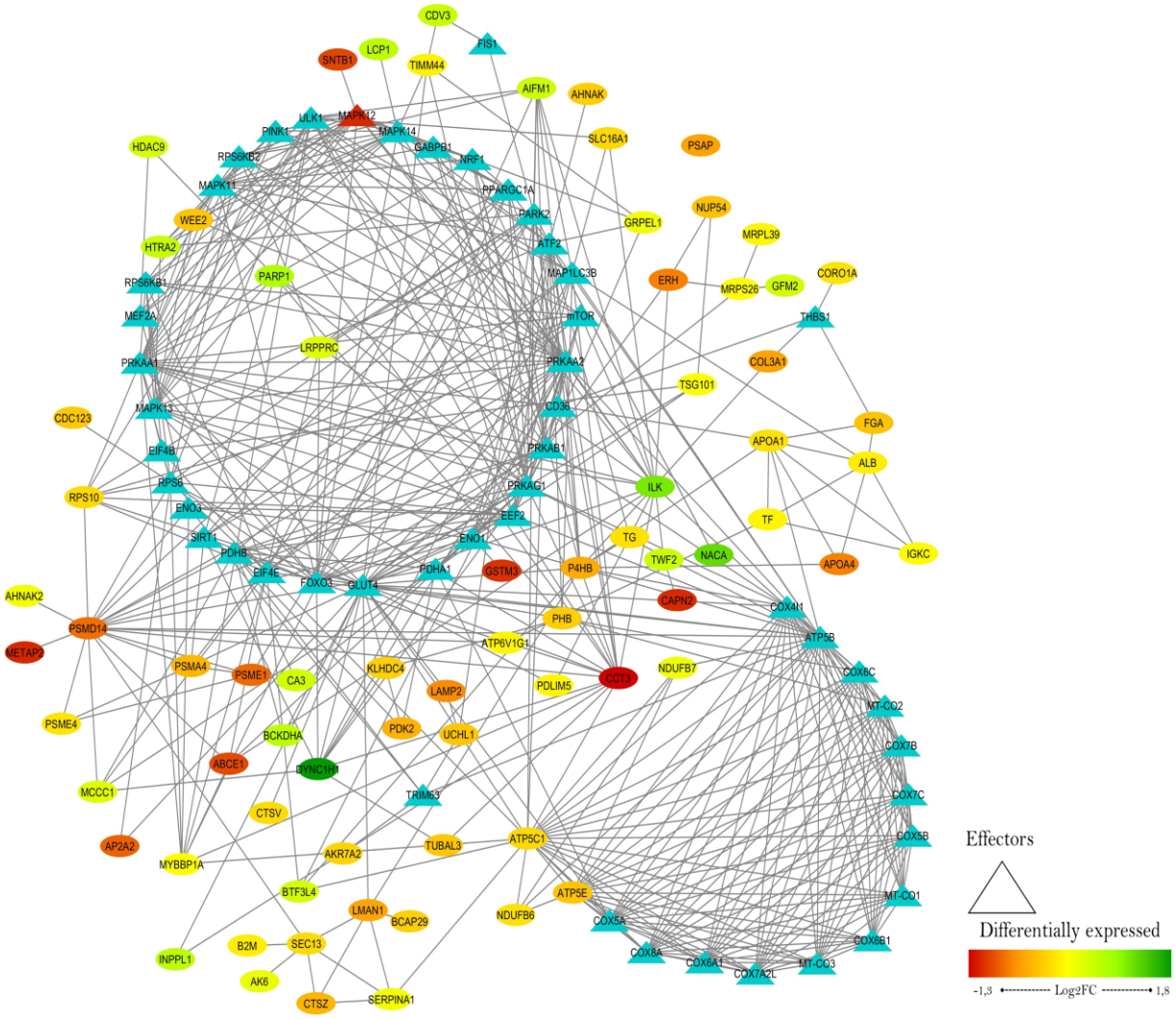

Figure 3. Visual protein interaction network map of the proteins significantly related to skeletal muscle adaptations to endurance exercise training according to the artificial neuronal network (ANN) score, and their interacting proteins, in wild-type (*wt/wt*) mice. The network map includes include three representations of the following interactions: i) within the differentially expressed proteins (ovals), ii) between the differentially expressed proteins and skeletal muscle adaptions to endurance exercise effectors (ovals and triangles), and iii) within the skeletal muscle adaptations to endurance exercise effectors (triangles).

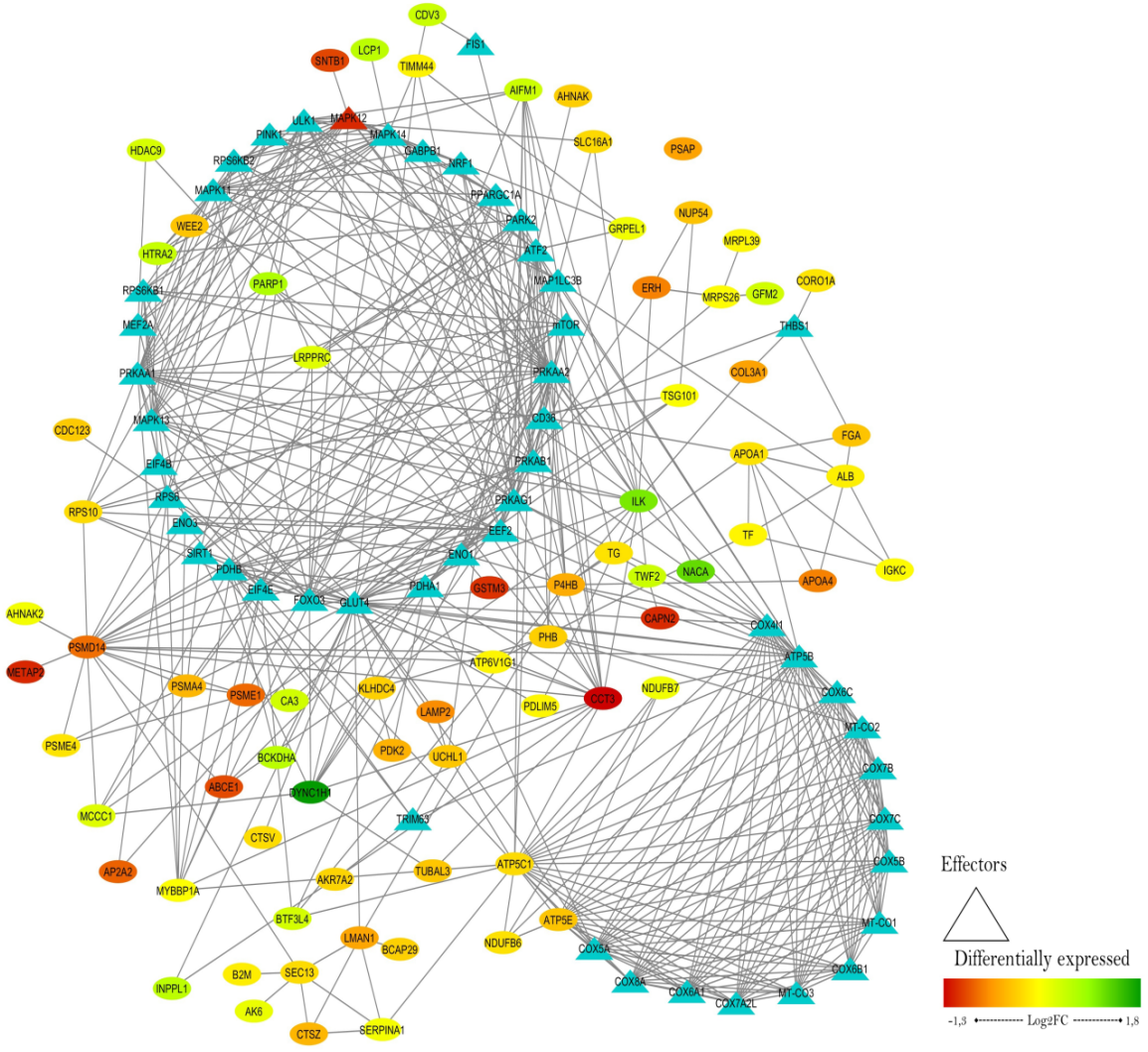

Figure 4. Integrative model summarising the main study findings. Abbreviations: LIMCH1, LIM and calponin homology domains-containing protein 1; MAPK12, mitogen-activated protein kinase 12; PARP1, poly [ADP-ribose] polymerase 1; TIGD4, tigger transposable element derived 4.

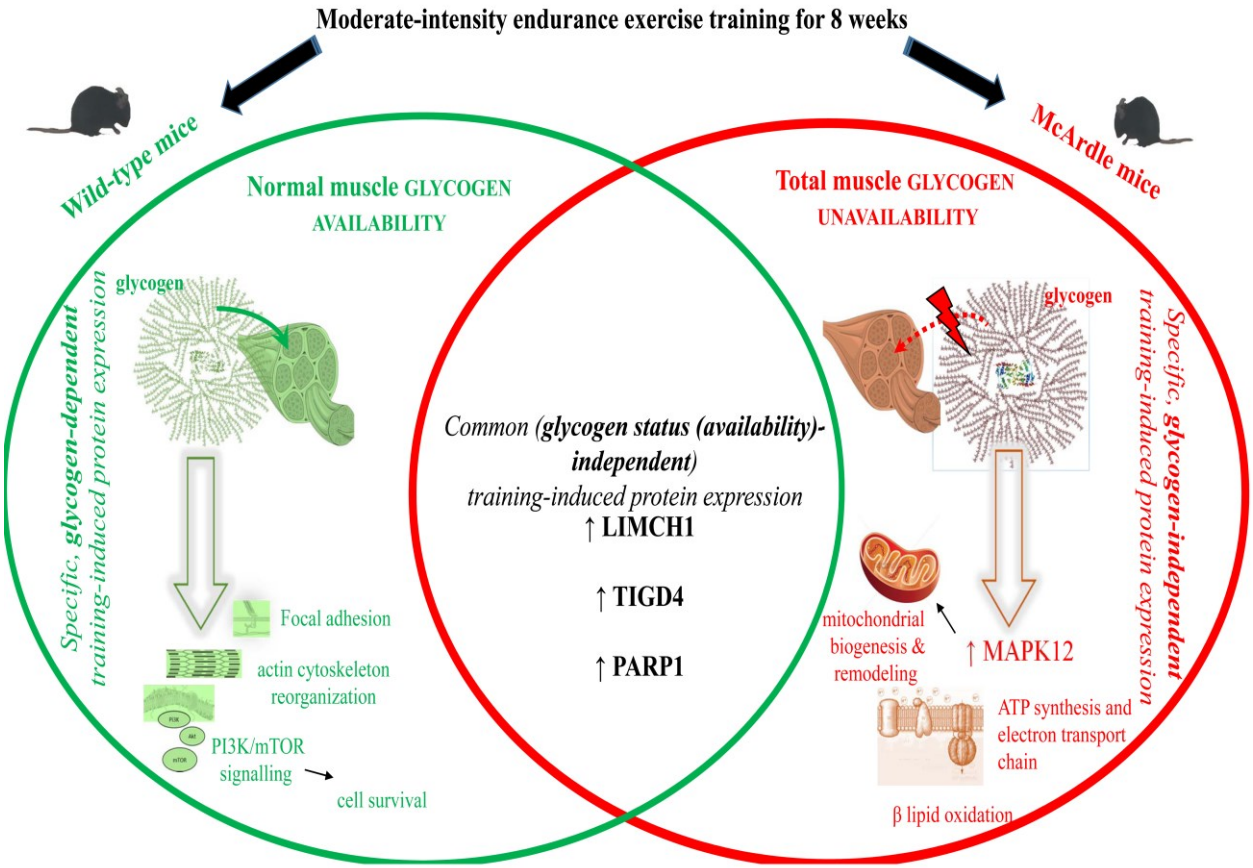

References

Altschul SF, Gish W, Miller W, Myers EW & Lipman DJ. (1990). Basic local alignment search tool. *J Mol Biol* **215,** 403-410.

Ayala JE, Bracy DP, James FD, Julien BM, Wasserman DH & Drucker DJ. (2009). The glucagon-like peptide-1 receptor regulates endogenous glucose production and muscle glucose uptake independent of its incretin action. *Endocrinology* **150,** 1155-1164.

Bartlett JD, Hawley JA & Morton JP. (2015). Carbohydrate availability and exercise training adaptation: too much of a good thing? *Eur J Sport Sci* **15,** 3-12.

Bassel-Duby R & Olson EN. (2006). Signaling pathways in skeletal muscle remodeling. *Annu Rev Biochem* **75,** 19-37.

Berenbaum MC. (1989). What is synergy? *Pharmacol Rev* **41,** 93-141.

Bergstrom J, Hermansen L, Hultman E & Saltin B. (1967). Diet, muscle glycogen and physical performance. *Acta Physiol Scand* **71,** 140-150.

Blake JA, Eppig JT, Kadin JA, Richardson JE, Smith CL, Bult CJ & the Mouse Genome Database G. (2017). Mouse Genome Database (MGD)-2017: community knowledge resource for the laboratory mouse. *Nucleic Acids Res* **45,** D723-D729.

Bonzon-Kulichenko E, Garcia-Marques F, Trevisan-Herraz M & Vazquez J. (2015). Revisiting peptide identification by high-accuracy mass spectrometry: problems associated with the use of narrow mass precursor windows. *J Proteome Res* **14,** 700-710.

.

Brull A, de Luna N, Blanco-Grau A, Lucia A, Martin MA, Arenas J, Marti R, Andreu AL & Pinos T. (2015). Phenotype consequences of myophosphorylase dysfunction: insights from the McArdle mouse model. *J Physiol* **593,** 2693-2706.

Cardona M, Lopez JA, Serafin A, Rongvaux A, Inserte J, Garcia-Dorado D, Flavell R, Llovera M, Canas X, Vazquez J & Sanchis D. (2015). Executioner Caspase-3 and 7 Deficiency Reduces Myocyte Number in the Developing Mouse Heart. *PLoS One* **10,** e0131411.

Cuenda A & Rousseau S. (2007). p38 MAP-kinases pathway regulation, function and role in human diseases. *Biochim Biophys Acta* **1773,** 1358-1375.

Favier FB, Benoit H & Freyssenet D. (2008). Cellular and molecular events controlling skeletal muscle mass in response to altered use. *Pflugers Arch* **456,** 587-600.

Fiuza-Luces C, Nogales-Gadea G, García-Consuegra I, Pareja-Galeano H, Rufián-Vázquez L, Pérez LM, Andreu AL, Arenas J, Martín MA, Pinós T, Lucia A, Morán M. (2016). Muscle signaling in exercise intolerance: Insights from the McArdle mouse model. *Med Sci Sports Exerc* **48,** 1448-1458.

Fiuza-Luces C, Soares-Miranda L, Gonzalez-Murillo A, Palacio JM, Colmenero I, Casco F, Melen GJ, Delmiro A, Moran M, Ramirez M & Lucia A. (2013). Exercise benefits in chronic graft versus host disease: a murine model study. *Med Sci Sports Exerc* **45,** 1703-1711.

Frolkis A, Knox C, Lim E, Jewison T, Law V, Hau DD, Liu P, Gautam B, Ly S, Guo AC, Xia J, Liang Y, Shrivastava S & Wishart DS. (2010). SMPDB: The Small Molecule Pathway Database. *Nucleic Acids Res* **38,** D480-487.

Frontera WR & Ochala J. (2015). Skeletal muscle: a brief review of structure and function. *Calcif Tissue Int* **96,** 183-195.

.

Garcia-Marques F, Trevisan-Herraz M, Martinez-Martinez S, Camafeita E, Jorge I, Lopez JA, Mendez-Barbero N, Mendez-Ferrer S, Del Pozo MA, Ibanez B, Andres V, Sanchez-Madrid F, Redondo JM, Bonzon-Kulichenko E & Vazquez J. (2016). A Novel Systems-Biology Algorithm for the Analysis of Coordinated Protein Responses Using Quantitative Proteomics. *Mol Cell Proteomics* **15,** 1740-1760.

Grundy D. (2015) Principles and standards for reporting animal experiments in The Journal of Physiology and Experimental Physiology. *J Physiol* **593,** 2547-2549.

Ha HC & Snyder SH. (1999). Poly(ADP-ribose) polymerase is a mediator of necrotic cell death by ATP depletion. *Proc Natl Acad Sci U S A* **96,** 13978-13982.

Haller RG, Wyrick P, Taivassalo T & Vissing J. (2006). Aerobic conditioning: an effective therapy in McArdle's disease. *Ann Neurol* **59,** 922-928.

Han H, Shim H, Shin D, Shim JE, Ko Y, Shin J, Kim H, Cho A, Kim E, Lee T, Kim H, Kim K, Yang S, Bae D, Yun A, Kim S, Kim CY, Cho HJ, Kang B, Shin S & Lee I. (2015). TRRUST: a reference database of human transcriptional regulatory interactions. *Sci Rep* **5,** 11432.

Herrando-Grabulosa M, Mulet R, Pujol A, Mas JM, Navarro X, Aloy P, Coma M & Casas C. (2016). Novel Neuroprotective Multicomponent Therapy for Amyotrophic Lateral Sclerosis Designed by Networked Systems. *PLoS One* **11,** e0147626.

Ho RC, Alcazar O, Fujii N, Hirshman MF & Goodyear LJ. (2004). p38gamma MAPK regulation of glucose transporter expression and glucose uptake in L6 myotubes and mouse skeletal muscle. *Am J Physiol Regul Integr Comp Physiol* **286,** R342-349.

.

Hoydal MA, Wisloff U, Kemi OJ & Ellingsen O. (2007). Running speed and maximal oxygen uptake in rats and mice: practical implications for exercise training. *Eur J Cardiovasc Prev Rehabil* **14,** 753-760.

Iborra-Egea O, Galvez-Monton C, Roura S, Perea-Gil I, Prat-Vidal C, Soler-Botija C & Bayes-Genis A. (2017). Mechanisms of action of sacubitril/valsartan on cardiac remodeling: a systems biology approach. *NPJ Syst Biol Appl* **3,** 12.

Isern J, Martin-Antonio B, Ghazanfari R, Martin AM, Lopez JA, del Toro R, Sanchez-Aguilera A, Arranz L, Martin-Perez D, Suarez-Lledo M, Marin P, Van Pel M, Fibbe WE, Vazquez J, Scheding S, Urbano-Ispizua A & Mendez-Ferrer S. (2013). Self-renewing human bone marrow mesenspheres promote hematopoietic stem cell expansion. *Cell Rep* **3,** 1714-1724.

Jungmichel S, Rosenthal F, Altmeyer M, Lukas J, Hottiger MO & Nielsen ML. (2013). Proteome-wide identification of poly(ADP-Ribosyl)ation targets in different genotoxic stress responses. *Mol Cell* **52,** 272-285.

Kanehisa M, Goto S, Sato Y, Kawashima M, Furumichi M & Tanabe M. (2014). Data, information, knowledge and principle: back to metabolism in KEGG. *Nucleic Acids Res* **42,** D199-205.

Koulmann N & Bigard AX. (2006). Interaction between signalling pathways involved in skeletal muscle responses to endurance exercise. *Pflugers Arch* **452,** 125-139.

Krag TO, Pinos T, Nielsen TL, Brull A, Andreu AL & Vissing J. (2016a). Differential muscle involvement in mice and humans affected by McArdle disease. *J Neuropathol Exp Neurol* **75,** 441–454.

Krag TO, Pinós T, Nielsen TL, Duran J, García-Rocha M, Andreu AL, Vissing J. (2016b). Differential glucose metabolism in mice and humans affected by McArdle disease. A*m J Physiol Regul Integr Comp Physiol* **311,** R307-R314.

Lane SC, Camera DM, Lassiter DG, Areta JL, Bird SR, Yeo WK, Jeacocke NA, Krook A, Zierath JR, Burke LM & Hawley JA. (2015). Effects of sleeping with reduced carbohydrate availability on acute training responses. *J Appl Physiol (1985)* **119,** 643-655.

Lin YH, Zhen YY, Chien KY, Lee IC, Lin WC, Chen MY & Pai LM. (2017). LIMCH1 regulates nonmuscle myosin-II activity and suppresses cell migration. *Mol Biol Cell* **28,** 1054-1065.

Lucia A, Nogales-Gadea G, Perez M, Martin MA, Andreu AL & Arenas J. (2008). McArdle disease: what do neurologists need to know? *Nat Clin Pract Neurol* **4,** 568-577.

Lucia A, Ruiz JR, Santalla A, Nogales-Gadea G, Rubio JC, Garcia-Consuegra I, Cabello A, Perez M, Teijeira S, Vieitez I, Navarro C, Arenas J, Martin MA & Andreu AL. (2012). Genotypic and phenotypic features of McArdle disease: insights from the Spanish national registry. *J Neurol Neurosurg Psychiatry* **83,** 322-328.

Martinez-Bartolome S, Navarro P, Martin-Maroto F, Lopez-Ferrer D, Ramos-Fernandez A, Villar M, Garcia-Ruiz JP & Vazquez J. (2008). Properties of average score distributions of SEQUEST: the probability ratio method. *Mol Cell Proteomics* **7,** 1135-1145.

Mate-Munoz JL, Moran M, Perez M, Chamorro-Vina C, Gomez-Gallego F, Santiago C, Chicharro L, Foster C, Nogales-Gadea G, Rubio JC, Andreu AL, Martin MA, Arenas J & Lucia A. (2007). Favorable responses to acute and chronic exercise in McArdle patients. *Clin J Sport Med* **17,** 297-303.

Navarro P, Trevisan-Herraz M, Bonzon-Kulichenko E, Nunez E, Martinez-Acedo P, Perez-Hernandez D, Jorge I, Mesa R, Calvo E, Carrascal M, Hernaez ML, Garcia F, Barcena JA, Ashman K, Abian J, Gil C, Redondo JM & Vazquez J. (2014). General statistical framework for quantitative proteomics by stable isotope labeling. *J Proteome Res* **13,** 1234-1247.

Navarro P & Vazquez J. (2009). A refined method to calculate false discovery rates for peptide identification using decoy databases. *J Proteome Res* **8,** 1792-1796.

Nogales-Gadea G, Pinos T, Lucia A, Arenas J, Camara Y, Brull A, de Luna N, Martin MA, Garcia-Arumi E, Marti R & Andreu AL. (2012). Knock-in mice for the R50X mutation in the PYGM gene present with McArdle disease. *Brain* **135,** 2048-2057.

Pache RA, Zanzoni A, Naval J, Mas JM & Aloy P. (2008). Towards a molecular characterisation of pathological pathways. *FEBS Lett* **582,** 1259-1265.

Pernow B & Saltin B. (1971). Availability of substrates and capacity for prolonged heavy exercise in man. *J Appl Physiol* **31,** 416-422.

Rivals I, Personnaz L, Taing L & Potier MC. (2007). Enrichment or depletion of a GO category within a class of genes: which test? *Bioinformatics* **23,** 401-407.

Russell AP. (2010). Molecular regulation of skeletal muscle mass. *Clin Exp Pharmacol Physiol* **37,** 378-384.

Santalla A, Nogales-Gadea G, Ortenblad N, Brull A, de Luna N, Pinos T & Lucia A. (2014). McArdle disease: a unique study model in sports medicine. *Sports Med* **44,** 1531-1544.

Sonnhammer EL & Ostlund G. (2015). InParanoid 8: orthology analysis between 273 proteomes, mostly eukaryotic. *Nucleic Acids Res* **43,** D234-239.

The UniProt C. (2017). UniProt: the universal protein knowledgebase. *Nucleic Acids Res* **45,** D158-D169.

Turk WR, Heller SL, Norris BJ & Nemeth PM. (1990). Increased muscular beta-hydroxyacyl CoA dehydrogenase with McArdle's disease. *Muscle Nerve* **13,** 607-612.

Vissing J & Haller RG. (2003). The effect of oral sucrose on exercise tolerance in patients with McArdle's disease. *N Engl J Med* **349,** 2503-2509.

Webster CC, Noakes TD, Chacko SK, Swart J, Kohn TA & Smith JA. (2016). Gluconeogenesis during endurance exercise in cyclists habituated to a long-term low carbohydrate high-fat diet. *J Physiol* **594,** 4389-4405.

Whirl-Carrillo M, McDonagh EM, Hebert JM, Gong L, Sangkuhl K, Thorn CF, Altman RB & Klein TE. (2012). Pharmacogenomics knowledge for personalized medicine. *Clin Pharmacol Ther* **92,** 414-417.

Table 1. McArdle (*p.R50X/p.R50X*) mice: Summary of the interactions found between the differentially expressed proteins (in exercise *vs.* control groups) and of the protein effectors of skeletal muscle adaptations to endurance exercise training

UniProt	Gene name	Effectors	No. of interactions	No. of interactions with effectors	No. of interacting effectors, **adaptive muscle growth**	interacting effectors, **mitochondrial biogenesis & remodelling**	NNo. of interacting effectors, **glucose & lipid metabolism adaptations**	interacting effectors, **angiogenesis**
P36542	*ATP5C1*		23	18	1	16	1	1
P53778	*MAPK12*	✗	19	15	4	12	0	3
P56381	*ATP5E*	✓	17	14	0	14	0	0
O00487	*PSMD14*	✗	18	9	2	4	3	0
Q13418	*ILK*	✗	17	9	1	7	1	1
P49368	*CCT3*	✗	12	9	3	5	1	1
		✗						

P07237	*P4HB*		11	8	0	6	2	1
O95831	*AIFM1*		8	8	2	6	0	0
P46783	*RPS10*		8	8	4	3	1	0
P09874	*PARP1*		8	7	0	7	0	0
Q14204	*DYNC1H1*		9	6	1	4	1	0
Q9BQG0	*MYBBP1A*		9	6	3	3	1	1
P0C1S8	*WEE2*		7	6	0	6	0	1
O43464	*HTRA2*		6	6	0	6	0	1
P42704	*LRPPRC*		6	6	4	3	0	1
P35232	*PHB*		6	5	0	4	1	1
P25789	*PSMA4*		6	3	0	2	1	0
Q96RQ3	*MCCC1*		4	3	1	0	2	0
O43615	*TIMM44*		4	3	0	2	1	0
Q99816	*TSG101*		4	3	1	0	2	0
Q9HAV7	*GRPEL1*		4	3	0	3	0	1
Q15119	*PDK2*		3	3	0	0	3	0
P02647	*APOA1*		8	2	0	1	1	0
P09936	*UCHL1*		3	2	1	1	0	0
Q96K17	*BTF3L4*		2	2	1	1	0	0
E9PAV3	*NACA*		2	2	0	2	0	1
P61221	*ABCE1*		2	2	1	1	0	0
P53985	*SLC16A1*		2	2	0	2	0	0
P12694	*BCKDHA*		2	2	0	0	2	0
O94973	*AP2A2*		2	2	1	0	1	0

P07451	*CA3*		2	2	0	0	2	0
P49257	*LMAN1*		6	1	0	0	1	0
P02768	*ALB*		6	1	0	1	0	0
Q06323	*PSME1*		4	1	0	1	0	0
P84090	*ERH*		4	1	0	1	0	0
P02671	*FGA*		3	1	0	0	0	1
P01266	*TG*		2	1	0	1	0	1
Q9UKY7	*CDV3*		2	1	0	1	0	0
O95139	*NDUFB6*		2	1	0	1	0	0
P02461	*COL3A1*		2	1	0	0	0	1
O15357	*INPPL1*		2	1	0	0	1	0
Q9BYN8	*MRPS26*		2	1	0	0	1	0
Q9UKV0	*HDAC9*		2	1	0	1	0	1
P13473	*LAMP2*		2	1	0	0	1	0
P31146	*CORO1A*		1	1	0	0	0	1
Q09666	*AHNAK*		1	1	0	1	0	1
P13796	*LCP1*		1	1	0	1	0	0
P21266	*GSTM3*		1	1	0	0	1	0
Q96HC4	*PDLIM5*		1	1	0	0	1	0
P17568	*NDUFB7*		1	1	0	1	0	0
O43488	*AKR7A2*		1	1	1	0	0	0
O60911	*CTSV*		1	1	0	0	1	0
O75794	*CDC123*		1	1	1	0	0	0
Q13884	*SNTB1*		1	1	0	1	0	1

Symbols: non-effectors and effectors of skeletal muscle adaptations to endurance exercise training among the differentially expressed proteins.

Table 2. Wild-type (*wt*/*wt*) mice: Summary of the interactions found between the differentially expressed proteins (in exercise *vs.* control groups) and of the protein effectors of skeletal muscle adaptations to endurance exercise training

UniProt		Effectors		with effectors	No. of interacting effectors, **adaptive muscle growth**	**mitochondrial biogenesis & remodelling**	effectors, **glucose & lipid metabolism adaptations**	No. of interacting effectors, **angiogenesis**
P05388	*RPLP0*		15	13	5	7	1	0
P11940	*PABPC1*	✗	18	12	5	6	1	0
P78527	*PRKDC*	✗	16	12	3	9	0	1
P45985	*MAP2K4*	✗	14	11	2	9	0	1
Q16512	*PKN1*	✗	14	11	3	8	0	1
P46778	*RPL21*	✗	10	9	5	4	0	0
P62879	*GNB2*	✗	9	8	1	6	1	3
Q562R1	*ACTBL2*	✗	8	8	1	7	0	0
		✗						

P09874	*PARP1*		9	7	0	7	0	0
P15056	*BRAF*	☒	9	7	1	6	0	1
P35544	*FAU*	☒	10	6	4	2	0	0
P42677	*RPS27*	☒	11	5	4	0	1	0
P16520	*GNB3*	☒	6	5	1	4	0	1
P56192	*MARS*	☒	6	5	1	4	0	0
P08195	*SLC3A2*	☒	5	5	1	3	1	1
P06737	*PYGL*	☒	5	4	1	2	1	0
P62140	*PPP1CB*	☒	6	3	0	1	2	1
O76094	*SRP72*	☒	6	2	1	0	1	0
Q99972	*MYOC*	☒	4	2	0	0	2	0
Q13683	*ITGA7*	☒	2	2	0	0	1	1
Q6PKG0	*LARP1*	☒	2	2	0	2	0	0
O75815	*BCAR3*	☒	4	1	0	1	0	0
P07951	*TPM2*	☒	2	1	0	0	1	0
P26012	*ITGB8*	☒	2	1	0	0	0	1
Q13409	*DYNC1I2*	☒	2	1	0	0	1	0
Q15631	*TSN*	☒	2	1	0	1	0	0
O95302	*FKBP9*	☒	1	1	0	0	1	0
P07108	*DBI*	☒	1	1	0	1	0	0
Q13564	*NAE1*	☒	1	1	0	1	0	0
Q13936	*CACNA1C*	☒	1	1	0	1	0	0
Q5VZF2	*MBNL2*	☒	1	1	0	0	1	0
Q5XPI4	*RNF123*	☒	1	1	0	1	0	0
		☒						

Q8WUD1	*RAB2B*		1	1	0	1	0	1
Q9HA65	*TBC1D17*		1	1	0	1	0	0

Symbol: Non effectors of skeletal muscle adaptations to exercise training among the differentially expressed proteins.

.

Table 3. Differentially expressed proteins significantly linked to skeletal muscle adaptations in McArdle and wild-type mice. The higher the artificial neuronal network (ANN) predictive score, the stronger is the relationship between the protein and skeletal muscle adaptations to endurance exercise training or its motives.

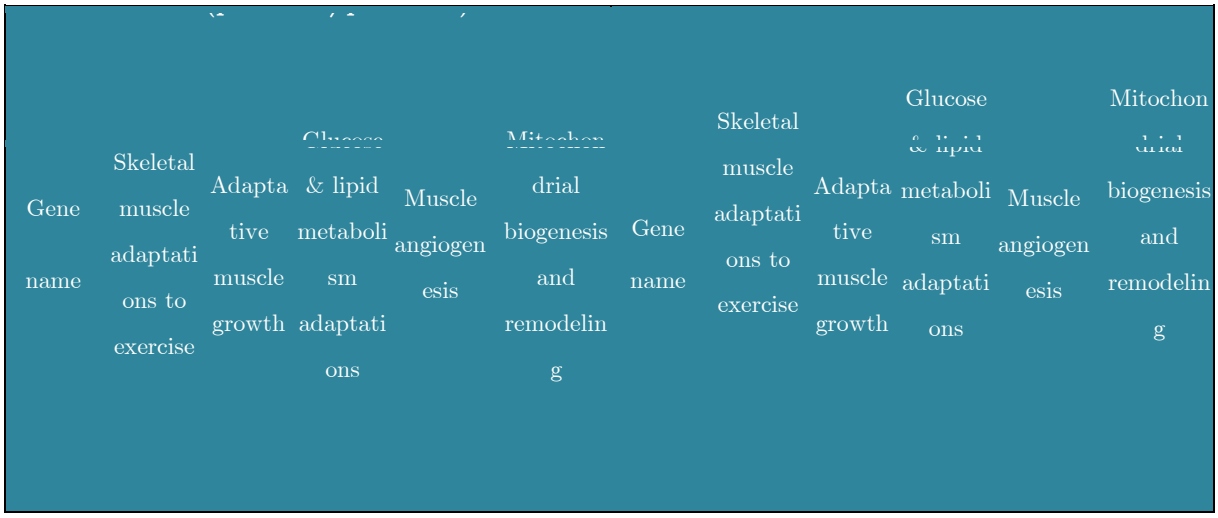

APOA1	88%	5%	68%	17%	65 %	LARP1	72%	13%	15%	16%	14 %
MAPK12	84%	52%	5%	64%	92 %	DYNC1I2	71%	5%	10%	16%	52 %
CDV3	77%	16%	14%	6%	74 %	PARP1	71%	37%	19%	27%	71 %
LRPPRC	77%	70%	5%	67%	37 %	BRAF	70%	5%	13%	62%	65 %
TSG101	75%	61%	5%	11%	58 %	GNB2	69%	27%	70%	55%	70 %
ERH	72%	5%	14%	11%	54 %	INCENP	67%	5%	5%	5%	23 %
PARP1	71%	37%	19%	27%	71 %	CUTA	63%	5%	12%	16%	16 %
CAPN2	71%	5%	17%	5%	67 %	UBE2V2	63%	5%	5%	16%	11 %
CORO1A	71%	5%	5%	64%	49 %	GNB3	57%	12%	5%	68%	64 %
DYNC1H1	71%	33%	5%	24%	31 %	MYOC	57%	5%	68%	5%	5 %
PDK2	71%	5%	64%	18%	14 %	CACNA1C	54%	13%	15%	17%	65 %
CA3	71%	15%	66%	18%	5 %	ASB15	53%	6%	5%	16%	64 %
PHB	70%	8%	5%	5%	26 %	PPP1CB	48%	17%	5%	65%	18 %
TF	70%	6%	5%	16%	15 %	APOH	44%	6%	16%	5%	25 %
AIFM1	70%	5%	8%	5%	14 %	NAE1	43%	5%	7%	16%	5 %
HTRA2	69%	18%	5%	16%	48 %	MYH11	41%	15%	7%	5%	5 %

PSMD1	68%	6%	6%	6%	58 %	TSN	29%	15%	16%	16%	44 %
4											
B2M	67%	7%	5%	11%	14 %	RPL21	22%	59%	6%	16%	5 %
ALB	65%	9%	8%	11%	48 %	FAU	19%	60%	6%	16%	48 %
SERPI	65%	5%	5%	5%	48 %	RPLP0	17%	56%	5%	16%	34 %
NA1											
GSTM3	64%	5%	6%	16%	40 %	SRP72	17%	36%	67%	5%	50%
HDAC9	64%	6%	6%	69%	38 %	-	-	-	-	-	-
AK6	63%	6%	5%	16%	13 %	-	-	-	-	-	-
MYBB	61%	69%	5%	66%	26 %	-	-	-	-	-	-
P1A											
FGA	61%	6%	10%	16%	5 %	-	-	-	-	-	-
AP2A2	55%	32%	16%	11%	5 %	-	-	-	-	-	-
PSAP	54%	5%	8%	6%	5 %	-	-	-	-	-	-
P4HB	53%	15%	5%	16%	55 %	-	-	-	-	-	-
CCT3	48%	28%	5%	11%	65 %	-	-	-	-	-	-
UCHL1	45%	16%	5%	16%	40 %	-	-	-	-	-	-
ATP5C	44%	5%	5%	5%	55 %	-	-	-	-	-	-
1											
ATP5E	42%	5%	13%	10%	53 %	-	-	-	-	-	-
LMAN1	42%	5%	5%	16%	5 %	-	-	-	-	-	-
NDUFB	39%	5%	16%	7%	47 %	-	-	-	-	-	-
7											

PSMA4	35%	6%	17%	18%	51 %	-	-	-	-	-	-
NDUFB6	30%	6%	16%	11%	48 %	-	-	-	-	-	-
SEC13	28%	6%	8%	5%	62 %	-	-	-	-	-	-
MTM1	25%	23%	5%	10%	59 %	-	-	-	-	-	-
IGKC	23%	9%	5%	19%	57 %	-	-	-	-	-	-
LAMA5	22%	16%	15%	7%	50 %	-	-	-	-	-	-
RPS10	19%	59%	8%	16%	18 %	-	-	-	-	-	-
TUBAL3	18%	5%	7%	16%	64%	-	-	-	-	-	-

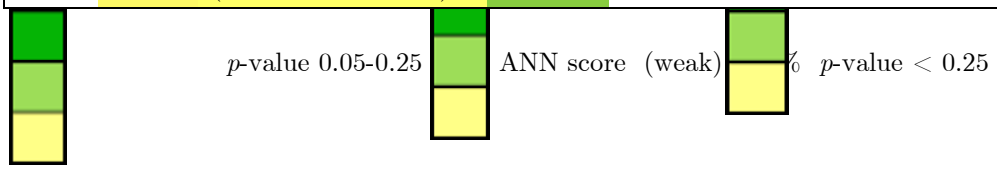

Appendix

Part 1. Summary of skeletal muscle adaptations to endurance exercise training through the review of specialised scientific literature

MOTIVE ID		(Short Name)
	40S ribosomal protein S6	RPS6 (rpS6)
Adaptive muscle growth	E3 ubiquitin-protein ligase TRIM63	TRIM63
	Elongation factor 2	EEF2
	Eukaryotic translation initiation factor 4B	IF4B
	Eukaryotic translation initiation factor 4E	EIF4E (eIF4E)
	Eukaryotic translation initiation factor 4E-binding protein 1	EIF4EBP1 (4EBP1)
	Forkhead box protein O3	FOXO3
	Growth/differentiation factor 8	MSTN
	Mechanistic target of rapamycin	mTOR
	Peroxisome proliferator-activated receptor gamma coactivator 1-alpha	PGC-1-alpha

	Phospholipase D1	PLD1
	Phospholipase D2	PLD2
	Ribosomal protein S6K 1	RPS6KB1
	Ribosomal protein S6K 2	(p70S6K1) RPS6KB2
	Cyclic AMP-dependent transcription factor	(p70S6K2) ATF2
	ATF-2	
	Mitogen-activated protein kinase 12	MAPK12 (p38g)
	Myocyte-specific enhancer factor 2A	MEF2A (MEF2)
Angiogenesis	Nitric oxide synthase, endothelial	NOS3
	Peroxisome proliferator-activated receptor	PGC-1-alpha
	gamma coactivator 1-alpha	
	Steroid hormone receptor ERR1	ESRRA (ERRa)
	Thrombospondin-1	TSP-1
	Vascular endothelial growth factor A	VEGFA
	Alpha-enolase	ENO1
Glucose and lipid metabolism	Beta-enolase	ENO3

adaptations	Carnitine O-palmitoyltransferase 1,	CPT1B
	muscle isoform	
	Fatty acid-binding protein, heart	FABP3
		(FABPH)
	Glycogen phosphorylase, muscle form	PYGM
	Glyoxalase I (Lactoylglutathione lyase)	GLO1
	Muscle form hexokinase	HK2
	Muscle-type aldolase	ALDOA
	Platelet glycoprotein 4	FAT/CD36
	Pyruvate dehydrogenase E1 component	
	subunit alpha, somatic form,	PDHA1
	mitochondrial	(PDHa)
	Pyruvate dehydrogenase E1 component	PDHB (PDHb)
	subunit beta, mitochondrial	
	Solute carrier family 2, facilitated glucose	SLC2A4
	transporter member 4	(GLUT4)
	5-aminolevulinate synthase, nonspecific,	ALAS1
Mitochondrial	mitochondrial	
biogenesis and	5'-AMP-activated protein kinase catalytic	PRKAA1
remodelling	subunit alpha-1	(AMPKa1)

5'-AMP-activated protein kinase catalytic subunit alpha-2	PRKAA1 (AMPKa2)
5'-AMP-activated protein kinase subunit beta-1	PRKAB1 (AMPKb)
5'-AMP-activated protein kinase subunit gamma-1	PRKAG1 (AMPKg)
ATP synthase subunit beta, mitochondrial	ATP5B
BCL2/adenovirus E1B 19 kDa protein-interacting protein 3	BNIP3
BCL2/adenovirus E1B 19 kDa protein-interacting protein 3-like	BNIP3L
Cyclic AMP-dependent transcription factor ATF-2	ATF2
Cytochrome c oxidase subunit 1	MT-CO1
Cytochrome c oxidase subunit 2	MT-CO2
Cytochrome c oxidase subunit 3	MT-CO3
Cytochrome c oxidase subunit 4 isoform 1, mitochondrial	COX4I1

2, mitochondria

Cytochrome c oxidase subunit 5A,	COX5A
mitochondrial Cytochrome c oxidase subunit 5B,	COX5B
mitochondrial Cytochrome c oxidase subunit 6A1,	Cox6a1
mitochondrial Cytochrome c oxidase subunit 6A2,	Cox6a2
mitochondrial Cytochrome c oxidase subunit 6B1	Cox6b1
Cytochrome c oxidase subunit 6B2	Cox6b2
Cytochrome c oxidase subunit 6C	Cox6c
Cytochrome c oxidase subunit 7A-related	Cox7r
protein, mitochondrial Cytochrome c oxidase subunit 7A1,	Cox7a1
mitochondrial Cytochrome c oxidase subunit 7A2,	Cox7a2
mitochondrial Cytochrome c oxidase subunit 7B,	Cox7b

mitochondrial	
Cytochrome c oxidase subunit 7C,	Cox7c
mitochondrial Cytochrome c oxidase subunit 8A,	Cox8a
mitochondrial P Cytochrome c oxidase subunit 8C,	Cox8c
mitochondrial E3 ubiquitin-protein ligase parkin	PARK2
	(PARKIN)
FUN14 domain-containing protein 1	FUNDC1
Microtubule-associated proteins 1A/1B	MAP1LC3B
light chain 3B	(LC3)
Mitochondrial fission 1 protein	FIS1
Mitofusin-1	MFN1
Mitofusin-2	MFN2
Mitogen-activated protein kinase 11	MAPK11
	(p38b)
Mitogen-activated protein kinase 12	MAPK12
	(p38g)

Mitogen-activated protein kinase 13	MAPK13
	(p38d)
Mitogen-activated protein kinase 14	MAPK14
	(p38a)
Myocyte-specific enhancer factor 2A	MEF2A (MEF2
	)
NAD-dependent protein deacetylase	SIRT1
sirtuin-1	
Nuclear respiratory factor 1	NRF-1
Nuclear respiratory factor 2 (GA-binding	NRF-2
protein subunit beta-1)	
Peroxisome proliferator-activated	PGC-1-alpha
receptor gamma coactivator 1-alpha	
PTEN-induced putative kinase protein 1	PINK1
Putative cytochrome c oxidase subunit	Cox7a3
7A3, mitochondrial	
Serine/threonine-protein kinase ULK1	ULK1 (ATG1)
Steroid hormone receptor ERR1	ESRRA
	(ERRa)

	Transcription factor A, mitochondrial	TFAM

Part 2. Summary of training loads in the two exercise groups (McArdle and wild-type) during the endurance exercise training program.

Training load variable	**Week 1 (5 sessions)**	**Week 2 (5 sessions)**	**Week 3 (5 sessions)**	**Week 4 (5 sessions)**	**Week 5 (5 sessions)**	**Week 6 (5 sessions)**	**Week 7 (5 sessions)**	**Week 8 (3 sessions)**
Intensity (%)*	55 (50, 60)	56 (50, 60)	61 (55, 65)	60 (50, 70)	59 (50, 65)	65 (55, 70)	66 (55, 75)	62 (50, 75)
Treadmill inclination (%)	0%	3 (0, 5)	9 (5, 15)	9 (5, 15)	13 (10, 15)	14 (10, 15)	14 (10, 15)	12 (5, 15)

Session duration (min)	32 (30, 35)	35 (30, 40)	41 (35, 45)	40 (40, 40)	43 (35, 50)	44 (35, 50)	45 (40, 50)	40 (30, 50)
Distance/session (McArdle, meters)	227 (207, 255)	264 (219, 305)	328 (292, 364)	337 (324, 362)	341 (280, 386)	372 (349, 412)	389 (261, 462)	396 (219, 455)
Distance/session (wild-type, meters)	303 (277, 344)	339 (283, 392)	423 (371, 473)	432 (385, 447)	440 (355, 492)	446 (434, 471)	463 (383, 481)	468 (411, 493)

Data are mean and range (min, max) for the core part of all the sessions within each week. * determined as % of the velocity reached at the end of the maximal performance test performed at the start of the study (abbreviated as V_{max} in the text). Of note, training loads decreased in the two days of the 8th week (Wednesday and Thursday) that preceded the final performance test (Friday).

Part 3. List of the differentially expressed proteins between the trained and sedentary McArdle mice (n=123) and the trained and sedentary wild-type mice (n= 74)

McArdle mice			Wild-type mice		
Mouse UniProt ID	**Uniprot ID**	**Gene Name**	**UniProt ID**	**Uniprot ID**	**Gene Name**
O08710	P01266	TG	P28028	P15056	BRAF
O08529	P17655	CAPN2	Q9QZK2	O75815	BCAR3
F6TQW2	-	-	B1ATL6	P45985	MAP2K4
Q8VCP8	Q9Y3D8	AK6	Q99LH9	Q7L8J4	SH3BP5L
Q5HZY7	O75348	ATP6V1G1	E0CXQ2	P0CG20	PRR35
Q9Z0P5	Q6IBS0	TWF2	Q3UK27	Q13564	NAE1
Q5SSW2	Q14997	PSME4	Q8BFZ3	Q562R1	ACTBL2
Q9DC11	Q6UX71	PLXDC2	Q9D404	Q9NWU1	OXSM
Q9JHU4	Q14204	DYNC1H1	O09167	P46778	RPL21
Q8CHH9	Q92599	SEPT8	Q920Q6	Q96DH6	MSI2
Q5RKZ7	Q9NZB8	MOCS1	P47802	Q13505	MTX1
Q545F5	P56381	ATP5E	Q54AE3	P16520	GNB3
P48774	P21266	GSTM3	P59279	Q8WUD1	RAB2B
P70670	E9PAV3	NACA	Q9WU62	Q9NQS7	INCENP
Q9Z0X1	O95831	AIFM1	P62880	P62879	GNB2
Q99LP6	Q9HAV7	GRPEL1	O08638	P35749	MYH11

D3YUB6	Q5XKL5	BTBD8	Q5M8R8	P05388	RPLP0
O08663	P50579	METAP2	Q9ET01	P06737	PYGL
Q61838	P20742	PZP	Q8BUZ3	Q8IY51	TIGD4
Q8C5W0	Q96JQ2	CLMN	Q8VHS6	Q8WXK1	ASB15
P01864	-	-	A2BFF7	Q13409	DYNC1I2
P01887	P61769	B2M	Q99K23	Q9NUQ7	UFSP2
Q3UX10	A6NHL2	TUBAL3	Q6ZQ58	Q6PKG0	LARP1
A0A0A6YW72	Q6V1P9	DCHS2	Q80X76	-	-
P08121	P02461	COL3A1	Q8BGF0	O00534	VWA5A
O88196	P53804	TTC3	O35206	P39059	COL15A1
P01837	P01834	IGKC	P21845	Q15661	TPSAB1
P97371	Q06323	PSME1	Q5XPI3	Q5XPI4	RNF123
Q4VAA2	Q9UKY7	CDV3	Q62348	Q15631	TSN
Q14C59	Q86T26	TMPRSS11B	Q9D2M8	Q15819	UBE2V2
Q921I1	P02787	TF	E9Q740	O76094	SRP72
Q9R1P0	P25789	PSMA4	Q9CQ89	O60888	CUTA
P05213	P68363	TUBA1B	E9PYH6	O15047	SETD1A
P84089	P84090	ERH	Q01815	Q13936	CACNA1C
Q3U1N0	P31146	CORO1A	Q8BL65	Q6H8Q1	ABLIM2
Q8R0Y8	Q86VD7	SLC25A42	P62862	P35544	FAU
Q5M9K7	P46783	RPS10	Q9D7X8	O75223	GGCT

Q9CQH7	Q96K17	BTF3L4	P28650	Q8N142	ADSSL1

Q8R404	Q5XKP0	MIC13	G3X9Q1	Q13683	ITGA7
O35857	O43615	TIMM44	P97822	Q9BTT0	ANP32E
P01867	-	-	A6H6K1	Q9BXN1	ASPN
Q9R0P9	P09936	UCHL1	P11103	P09874	PARP1
Q4VAE3	Q6PI78	TMEM65	Q60718	Q99965	ADAM2
Q6P549	O15357	INPPL1	P10852	P08195	SLC3A2
F6ZAP6	-	-	Q0VBD0	P26012	ITGB8
P62984	P62987	UBA52	P62141	P62140	PPP1CB
O09174	Q9UHK6	AMACR	P29341	P11940	PABPC1
E9PYB0	Q8IVF2	AHNAK2	Q8C4G9	Q86SQ6	ADGRA1
Q811B1	Q86Y38	XYLT1	Q8C0K5	P16260	SLC25A16
Q80ZW2	Q8WUY1	THEM6	Q3UH68	Q9UPQ0	LIMCH1
Q9D0F3	P49257	LMAN1	Q69ZX8	O94929	ABLIM3
E9Q616	Q09666	AHNAK	P97313	P78527	PRKDC
Q9WUU7	Q9UBR2	CTSZ	P31786	P07108	DBI
P09103	P07237	P4HB	Q01339	P02749	APOH
P16015	P07451	CA3	Q8VED9	Q3ZCW2	LGALSL
O35593	O00487	PSMD14	Q6R0H7	O95467	GNAS
Q542A1	Q9UHQ4	BCAP29	A2AIM4	P07951	TPM2
Q9EQZ7	Q9UQ26	RIMS2	Q9CXJ4	Q9NUT2	ABCB8
Q9Z2C5	Q13496	MTM1	Q8C181	Q5VZF2	MBNL2

Q8R092	Q9BWL3	C1orf43	Q6ZWU9	P42677	RPS27
Q99J47	Q6IAN0	DHRS7B	Q9EPM5	Q9H7C4	SYNC
Q546G4	P02768	ALB	P70268	Q16512	PKN1
Q80ZS3	Q9BYN8	MRPS26	Q6IRU7	Q5JTW2	CEP78
P61222	P61221	ABCE1	Q8CHG3	Q8IWJ2	GCC2
Q8CI51	Q96HC4	PDLIM5	Q32NZ6	Q6UXY8	TMC5
A2AE45	-	-	Q1XH17	Q6ZMU5	TRIM72
Q9D1M0	P55735	SEC13	Q9Z247	O95302	FKBP9
Q99NB1	Q9NUB1	ACSS1	Q62205	Q15858	SCN9A
Q8BUZ3	Q8IY51	TIGD4	Q8BG95	O60237	PPP1R12B
Q62087	Q15166	PON3	B0QZF7	Q8NCQ7	PROCA1
O88492	Q96Q06	PLIN4	Q8BYH7	Q9HA65	TBC1D17
O55222	Q13418	ILK	P11627	P32004	L1CAM
Q3V1H3	Q6MZM0	HEPHL1	O70624	Q99972	MYOC
Q3U4U6	P49368	CCT3	E9QB02	P56192	MARS
Q9JIY5	O43464	HTRA2			
P06728	P06727	APOA4			
Q544H9	Q96T49	PPP1R16B			
P53986	P53985	SLC16A1			
A3KGG4	A7MBM2	DISP2			
Q61207	P07602	PSAP			

Q9JKF7	Q9NYK5	MRPL39

P06330	-	-
Q8R2Q4	Q969S9	GFM2
Q9JK42	Q15119	PDK2
Q9CR61	P17568	NDUFB7
Q8CG76	O43488	AKR7A2
Q6PB66	P42704	LRPPRC
P50136	P12694	BCKDHA
O08911	P53778	MAPK12
Q1RLL3	Q8IYJ1	CPNE9
Q8C2K5	Q86YV0	RASAL3
Q80YR9	Q8IXT5	RBM12B
Q4FJQ6	P35237	SERPINB6
Q61001	O15230	LAMA5
Q61187	Q99816	TSG101
Q8K3C3	Q8WZA0	LZIC
P06797	O60911	CTSV
A2AAJ9	Q5VST9	OBSCN
Q3UZA1	Q6JBY9	RCSD1
Q99N13	Q9UKV0	HDAC9
Q8BGK2	Q8NDY3	ADPRHL1
P67778	P35232	PHB

P17047	P13473	LAMP2
D3YX79	-	-
Q8CII2	O75794	CDC123
E9PV24	P02671	FGA
P17427	O94973	AP2A2
Q99L88	Q13884	SNTB1
P11103	P09874	PARP1
Q9JHL1	Q15599	SLC9A3R2
Q3U2W2	Q9BQG0	MYBBP1A
Q9WV96	Q9Y5J6	TIMM10B
Q66JT0	P0C1S8	WEE2
A2AKU9	P36542	ATP5C1
A2AP31	O95139	NDUFB6
P33173	Q12756	KIF1A
Q921I2	Q8TBB5	KLHDC4
Q8BTS4	Q7Z3B4	NUP54
D3YU22	Q9UPQ0	LIMCH1
Q61233	P13796	LCP1
P22599	P01009	SERPINA1
Q99MR8	Q96RQ3	MCCC1
Q00623	P02647	APOA1

.

Part 4. Number of proteins reported for each artificial neuronal network (ANN) category in relation to skeletal muscle adaptations to endurance exercise training in McArdle and wild-type mice. Information is given for proteins individually ('individual'), in combination ('combined') and both ('total')

ANN Category	McArdle					Wild-type					Common
	Individual	%	Combi	%	Total %	Individual	%	Combi	%	Total %	proteins
Strong (p<0.05)	4	4%	135	2%	139	0	0%	1	0%	1	0
Medium-strong (p=0.05–0.25)	29	25%	1900	34 %	1 929 33%	16	22%	718	32 %	734	1
Weak (p>0.25)	78	67%	3 636	64 %	3 714 64%	52	71%	1 559	68 %	1 611 69%	2
Not assessed	5	4%	0	0%	5	5	7%	0	0%	5	0

Total	116	100%	5 671	100%	5 787	100%	100%	2 278	100%	2 351	100%	3

Part 5. Summary of all the enriched protein sets (the corresponding database is also indicated)

Source	McArdle mice	Wild-type mice
BED	7	0
BED Motives	9	5
BED Pathways	5	3
GO Function	7	3
GO Location	35	1
GO Process	55	2
PharmGKB	2	1
TRRUST	1	0
KEGG	0	13
SMPDB	0	51

TOTAL	**121**	**79**

Abbreviations: BED, Biological Effectors Database; GO, Gene Ontology; KEGG, Kyoto Encyclopedia of Genes and Genomes; PharmGKB, Pharmacogenomics Knowledgebase; SMPDB, Small Molecule Pathway Database; TRRUST, Transcriptional Regulatory Relationships Unraveled by Sentence-based Text-mining database.

Part 6. Enriched protein sets related to mitochondrial function in McArdle mice

BED Pathways	Oxidative phosphorylation (OXPHOS)
GO Function ID	Proton-transporting ATP synthase activity, rotational mechanism
GO Location	Mitochondrial crista junction
GO Location	Mitochondrial inner membrane
GO Location	Mitochondrial intermembrane space
GO Location	Mitochondrial matrix
GO Location	Mitochondrial proton-transporting ATP synthase complex
GO Location	Mitochondrial proton-transporting ATP synthase complex, catalytic core F(1)
GO Location	Mitochondrion

GO Process	Mitochondrion organisation
GO Process	Protein targeting to mitochondrion
GO Process	Respiratory electron transport chain

Abbreviations: BED, Biological Effectors Database; GO, Gene Ontology;

Part 7. Enriched protein sets related to muscle structure and growth

GO Location	costamere
GO Location	cytoskeleton
GO Location	focal adhesion
GO Location	membrane
GO Location	actin filament
GO Process	cell-matrix adhesion
GO Process	integrin-mediated signaling pathway
GO Process	positive regulation of Rho protein signal transduction
GO Process	regulation of actin cytoskeleton organization
GO Process	mitotic cell cycle
GO Process	positive regulation of ubiquitin-protein ligase activity involved in regulation of mitotic cell cycle transition

GO Process	regulation of ubiquitin-protein ligase activity involved in mitotic cell cycle

Abbreviations GO, Gene Ontology.

Part 8. Summary of the enriched protein sets related to increase in muscle size and function, and neuromodulation

KEGG	04510 _Focal adhesión
KEGG	04810 _Regulation of actin cytoskeleton
KEGG	04151 _PI3K-Akt signalling pathway
BED Pathways	Gastrointestinal smooth muscle sustained contraction
BED Pathways	Smooth muscle relaxation
BED Pathways	Vascular smooth muscle contraction
KEGG	04270 _Vascular smooth muscle contraction
GO Function	poly(U) RNA binding
GO Function	translation activator activity
GO Process	small GTPase mediated signal transduction
GO Process	translational initiation
KEGG	03015 _mRNA surveillance pathway
BED Motives	Nervous impluse generation deffect

KEGG	04713 _Circadian entrainment
KEGG	04151 _PI3K-Akt signaling pathway
KEGG	04720 _Long-term potentiation
KEGG	04726 _Serotonergic synapse
KEGG	04727 _GABAergic synapse
KEGG	04728_Dopaminergic synapse

Abbreviations: BED, Biological Effectors Database; GO, Gene Ontology; KEGG, Kyoto Encyclopedia of Genes and Genomes.

Part 9. Summary of the enriched protein set related to catecholamine modulation within wild-type (*wt*/*wt*) mice. Set sources are also indicated

PHARMKB	[PA2024] Beta-agonist/beta-blocker pathway, pharmacodynamics	SMPDB	[SMP00367] Carvedilol action pathway
SMPDB	[SMP00296] Acebutolol action pathway	SMPDB	[SMP00368] Labetalol action pathway
SMPDB	[SMP00297] Alprenolol action pathway	SMPDB	[SMP00375] Verapamil action pathway
SMPDB	[SMP00298] Atenolol action pathway	SMPDB	[SMP00376] Amlodipine action pathway
SMPDB	[SMP00299] Betaxolol action pathway	SMPDB	[SMP00377] Felodipine action pathway
SMPDB	[SMP00300] Bisoprolol action pathway	SMPDB	[SMP00378] Isradipine action pathway
SMPDB	[SMP00301] Esmolol action pathway	SMPDB	[SMP00379] Nifedipine action pathway
SMPDB	[SMP00302] Metoprolol action pathway	SMPDB	[SMP00380] Nimodipine action pathway

SMPDB	[SMP00303] Nadolol action pathway	SMPDB	[SMP00381] Nisoldipine action pathway
SMPDB	[SMP00304] Oxprenolol action pathway	SMPDB	[SMP00382] Nitrendipine action pathway
SMPDB	[SMP00305] Penbutolol action pathway	SMPDB	[SMP00588] Muscle/heart contraction
SMPDB	[SMP00306] Pindolol action pathway	SMPDB	[SMP00619] Felodipine metabolism pathway
SMPDB	[SMP00307] Propranolol action pathway	SMPDB	[SMP00657] Bopindolol action pathway
SMPDB	[SMP00320] Intracellular signaling through adenosine receptor A2a and adenosine	SMPDB	[SMP00658] Carteolol action pathway
SMPDB	[SMP00321] Intracellular signaling through adenosine receptor A2b and adenosine	SMPDB	[SMP00659] Timolol action pathway
SMPDB	[SMP00323] Quinidine action pathway	SMPDB	[SMP00660] Sotalol action pathway
SMPDB	[SMP00324] Procainamide (antiarrhythmic) action pathway	SMPDB	[SMP00661] Epinephrine action pathway
SMPDB	[SMP00325] Disopyramide action pathway	SMPDB	[SMP00662] Dobutamine action pathway
SMPDB	[SMP00326] Fosphenytoin (antiarrhythmic) action pathway	SMPDB	[SMP00663] Isoprenaline action pathway
SMPDB	[SMP00328] Lidocaine (antiarrhythmic) action	SMPDB	[SMP00664] Arbutamine action pathway
SMPDB	[SMP00329] Mexiletine action pathway	SMPDB	[SMP00665] Amiodarone action pathway
SMPDB	[SMP00330] Tocainide action pathway	SMPDB	[SMP00666] Levobunolol action pathway
SMPDB	[SMP00331] Flecainide action pathway	SMPDB	[SMP00667] Metipranolol action pathway
SMPDB	[SMP00332] Ibutilide action pathway	SMPDB	[SMP00668] Bevantolol action pathway
SMPDB	[SMP00359] Diltiazem action pathway	SMPDB	[SMP00669] Practolol action pathway
SMPDB	[SMP00366] Nebivolol action pathway	SMPDB	[SMP00670] Bupranolol action pathway